

TAUT FOLIATIONS, POSITIVE 3-BRAIDS, AND THE L-SPACE CONJECTURE

SIDDHI KRISHNA

Abstract. We construct taut foliations in every closed 3-manifold obtained by r -framed Dehn surgery along a positive 3-braid knot K in S^3 , where $r < 2g(K) - 1$ and $g(K)$ denotes the Seifert genus of K . This confirms a prediction of the L-space Conjecture. For instance, we produce taut foliations in every non-L-space obtained by surgery along the pretzel knot $P(-2, 3, 7)$, and indeed along every pretzel knot $P(-2, 3, q)$, for q a positive odd integer. This is the first construction of taut foliations for every non-L-space obtained by surgery along an infinite family of hyperbolic L-space knots. Additionally, we construct taut foliations in every closed 3-manifold obtained by r -framed Dehn surgery along a positive 1-bridge braid in S^3 , where $r < g(K)$.

1. INTRODUCTION

The L-space Conjecture predicts a surprising relationship between Floer-homological, algebraic, and geometric properties of a closed 3-manifold Y :

Conjecture 1.1 (The L-space Conjecture [BGW13, Juh15]). *Suppose Y is an irreducible rational homology 3-sphere. Then the following are equivalent:*

- (1) Y is a non-L-space (i.e. the Heegaard Floer homology of Y is not “simple”),
- (2) $\pi_1(Y)$ is left-orderable, and
- (3) Y admits a taut foliation.

Work by many researchers fully resolves Conjecture 1.1 in the affirmative for graph manifolds [BC15, BC17, BGW13, BNR97, CLW13, EHN81, HRRW15, LS09]. Combining results of Ozsváth-Szabó, Bowden, and Kazez-Roberts proves that if Y admits a taut foliation, then Y is a non-L-space [OS04, Bow16, KR17]. Here, we investigate the converse.

One strategy for producing non-L-spaces is via Dehn surgery. A non-trivial knot $K \subset S^3$ is an **L-space knot** if *some* non-trivial surgery along K produces an L-space. Lens spaces are prominent examples of L-spaces, so any knot with a non-trivial surgery to a lens space (notably Berge knots [Ber18]) is an L-space knot. Berge-Gabai knots are the subclass of 1-bridge braids in S^3 admitting lens space surgeries [Gab90, Ber18], yet *every* 1-bridge braid is an L-space knot [GLV18].

In fact, if K is an L-space knot, *infinitely* many surgeries along K yield L-spaces. In particular, for a non-trivial positive knot $K \subset S^3$, the set of L-space surgery slopes is either $[2g(K) - 1, \infty) \cap \mathbb{Q}$, or the empty set [KMOS07, RR17, OS05]. Thus, r -framed Dehn surgery along *any* non-trivial positive knot K yields a non-L-space for all $r < 2g(K) - 1$. Conjecture

1.1 predicts these manifolds admit taut foliations. This viewpoint guides our treatment of Conjecture 1.1 for a special class of positive knots.

Theorem 1.2. *Let K be a knot in S^3 , realized as the closure of a positive 3-braid. Then for every $r < 2g(K) - 1$, the knot exterior $X_K := S^3 - \mathring{\nu}(K)$ admits taut foliations meeting the boundary torus T in parallel simple closed curves of slope r . Hence the manifold obtained by r -framed Dehn filling, $S_r^3(K)$, admits a taut foliation.*

Remark 1.3. *Theorem 1.2 can be reformulated as follows: for K and r as above, the manifold $S_r^3(K)$ admits a taut foliation, such that the core of the Dehn surgery is a closed transversal.*

A 3-stranded twisted torus knot is a knot obtained as the closure of $(\sigma_1 \sigma_2)^q (\sigma_2)^{2s}$, where q and s are positive integers, and σ_1, σ_2 are the standard Artin generators. Vafaee proved every 3-stranded twisted torus knot is an L-space knot [Vaf15]. Moreover, if an L-space knot admits a presentation as a 3-braid closure, then K is a twisted torus knot [LV14]. Thus, hyperbolic L-space knots are abundant among positive 3-braid closures. Applying Theorem 1.2 yields:

Corollary 1.4. *In Conjecture 1.1, (1) \iff (3) holds for all Dehn surgeries along an infinite family of hyperbolic L-space knots.* \square

Lidman and Moore proved pretzel knots specified by the parameters $P(-2, 3, q)$, for $q \geq 1$, q odd are the only L-space pretzel knots [LM16]. These pretzel knots are realized as closures of positive 3-braids (see Figure 5). Applying Theorem 1.2, we deduce:

Corollary 1.5. *Let K be an L-space pretzel knot in S^3 . Then for any r -framed surgery on K , the surgered manifold $Y = S_r^3(K)$ is a non-L-space $\iff Y$ admits a taut foliation.* \square

We note that Delman-Roberts recover Corollary 1.5 in forthcoming work [DR].

Example 1.6. The Fintushel-Stern pretzel knot $P(-2, 3, 7)$ is a hyperbolic knot in S^3 admitting lens space surgeries [FS80], hence is an L-space knot. It can be realized as a positive 3-braid closure in S^3 (see Figure 5). In Section 3, we explicitly construct the family of taut foliations meeting the boundary torus T in all rational slopes $r < 2g(K) - 1 = 9$.

Tran, generalizing work of Nie [Nie18], showed that for any K in an infinite subfamily \mathcal{F} of 3-stranded twisted torus knots, and $r \geq 2g(K) - 1$, $\pi_1(S_r^3(K))$ is not left-orderable [Tra18]. The L-space pretzel knots comprise a proper subset of \mathcal{F} . We conclude:

Corollary 1.7. *Suppose Y is obtained by r -framed Dehn surgery along K in S^3 , for K a 3-stranded twisted torus knot in \mathcal{F} , and $r \in \mathbb{Q}$. Then*

$$\pi_1(Y) \text{ is not left-orderable} \iff Y \text{ is an L-space} \iff Y \text{ does not admit a taut foliation.}$$

That is, (2) \implies (1) \iff (3) of Conjecture 1.1 holds for manifolds obtained by Dehn surgeries along knots in \mathcal{F} .

Our methods for proving Theorem 1.2 are constructive. Inspired by work of Roberts [Rob01a, Rob01b], we build **sink disk free** branched surfaces in fibered knot exteriors. By Li [Li02, Li03], these branched surfaces carry essential laminations. We first extend these laminations to taut foliations in knot exteriors, and then to taut foliations in surgered manifolds.

Conjecture 1.1 predicts Theorem 1.2 holds for any knot K realized as a positive braid closure, on any number of strands. Any such K is fibered; applying [Rob01b], $S_r^3(K)$ admits a taut foliation for any $r < 1$. An adaptation of our techniques partially closes the gap between Roberts' result and the prediction for 1-bridge braids in S^3 :

Theorem 1.8. *Let K be any 1-bridge braid in S^3 , i.e. K is a knot in S^3 , realized as the closure of a braid β on w strands, where*

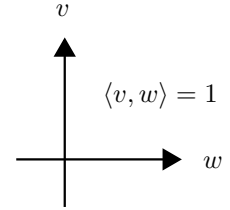
$$\beta = (\sigma_b \sigma_{b-1} \dots \sigma_2 \sigma_1)(\sigma_{w-1} \sigma_{w-2} \dots \sigma_2 \sigma_1)^t$$

for $w \geq 3, 1 \leq b \leq w-2, t \geq 1$. Then for every $r < g(K)$, the knot exterior $X_K := S^3 - \mathring{\nu}(K)$ admits taut foliations meeting the boundary torus T in parallel simple closed curves of slope r . Hence the manifold obtained by r -framed Dehn filling, $S_r^3(K)$, admits a taut foliation.

1.1. Organization. In Section 2, we review the required background on branched surfaces and fibered knots. In Section 3, we establish the foundations for proving Theorem 1.2. Along the way, we construct taut foliations for every $S_r^3(K)$, where $K = P(-2, 3, 7)$ and $r < 9$. In Section 4, we prove Theorem 1.2. In Section 5, we prove Theorem 1.8.

1.2. Conventions.

- We assume all braid closures are knots in S^3 .
- For any knot exterior X_K , $H_1(\partial X_K)$ is generated by the Seifert longitude λ and the standard meridian μ .
- Let $\langle \alpha, \beta \rangle$ denote the algebraic intersection number; following the sign convention above, we set $\langle \lambda, \mu \rangle = 1$. For any essential simple closed curve γ on $T = \partial X_K$, the slope of γ is determined by $\frac{\langle \gamma, \lambda \rangle}{\langle \mu, \gamma \rangle}$.
- We use $\sigma_1, \sigma_2, \dots, \sigma_{n-1}$ to represent the standard Artin generators for the n -stranded braid group. Strands are drawn vertically, oriented “down”, and enumerated from left-to-right. Given a braid diagram, we recover the braid word by reading β from top-to-bottom.
- Every surface F is orientable; in all figures of Seifert surfaces, only F^+ is visible.
- If a properly embedded arc α lies on F^- , it is drawn with a blue dotted line; if α lies on F^+ , it is drawn with a pink solid line. A helpful mnemonic: “pink” and “plus” both start with “p”.
- Given a fibered knot $K \subset S^3$ with fiber F and monodromy φ , the knot exterior is a mapping torus $F \times [0, 1] / \sim$, where $(x, 0) \sim (\varphi(x), 1)$. Moreover, $\varphi \approx \mathbb{1}$ in $\nu(\partial F)$.



1.3. Acknowledgements. I am grateful to my advisor, Josh Greene, for his guidance, patience, and kindness. Thanks to Tao Li for answering countless questions, and John Baldwin for sharing his vision to extend Roberts' results. Finally, thanks to Peter Feller, Kyle Hayden, and Patrick Orson for helpful conversations.

2. BACKGROUND

2.1. Branched Surfaces. Our primary tool for constructing taut foliations are branched surfaces. For a detailed exposition on branched surfaces, see Floyd-Oertel [FO84].

Definition 2.1. *A **spine for a branched surface** is a 2-complex in a 3-manifold M , locally modeled by:*

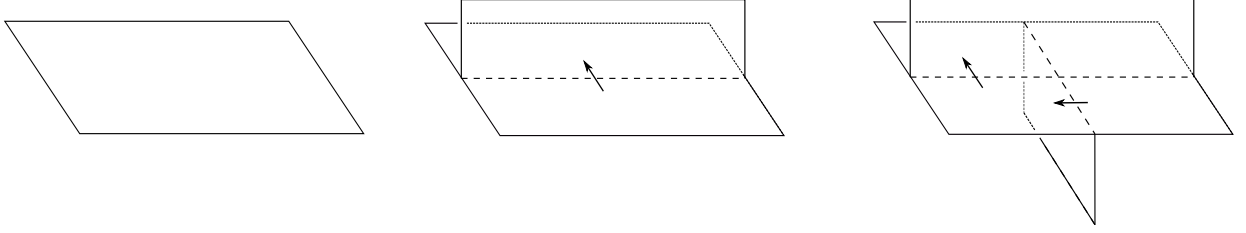


FIGURE 1. Ignoring the arrows yields the local models for the spine of a branched surface.

Definition 2.2. *A **branched surface** B in a 3-manifold M is built by providing smoothing/cusping instructions for a spine. It is locally modeled by:*

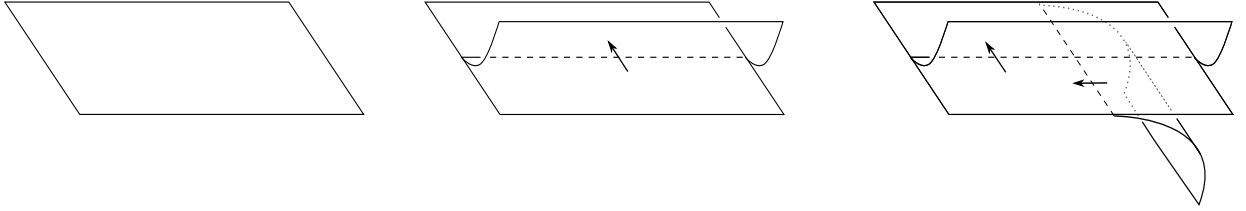


FIGURE 2. The cusping instructions for the spine in Figure 1 yield these local models.

A branched surface is locally homeomorphic to a surface everywhere except in a set of properly embedded arcs and simple closed curves, called the **branch locus** γ . A point p in γ is called a **triple point** if a neighborhood of p in B is locally modeled by the rightmost picture of Figure 2. A **branch sector** is a connected component of $\overline{B - \gamma}$ (the closure under the path metric). In this paper, all branched surfaces meet the boundary torus of X_K ; it will do so in a train track.

Definition 2.3. *A **sink disk** [Li02] is a branch sector S of B such that (1) S is homeomorphic to a disk, (2) $\partial S \cap \partial M = \emptyset$, and (3) the branch direction of every smooth arc or curve in its boundary points into the disk. A **half sink disk** [Li03] is a branch sector S of B such that (1) S is homeomorphic to a disk, and (2) $\partial S \cap \partial M \neq \emptyset$, and (3) the branch direction of each arc in $\partial S - \partial M$ points into S . Note: $\partial S \cap \partial M$ may not be connected. When a branched surface B contains no sink disk or half sink disk, we say B is **sink disk free**. See Figure 3.*

Thus, to prove a branched surface is sink disk free, we need only check that some cusped arc points out of each branch sector. Indeed, this is the heart of the proof of Theorem 1.2.

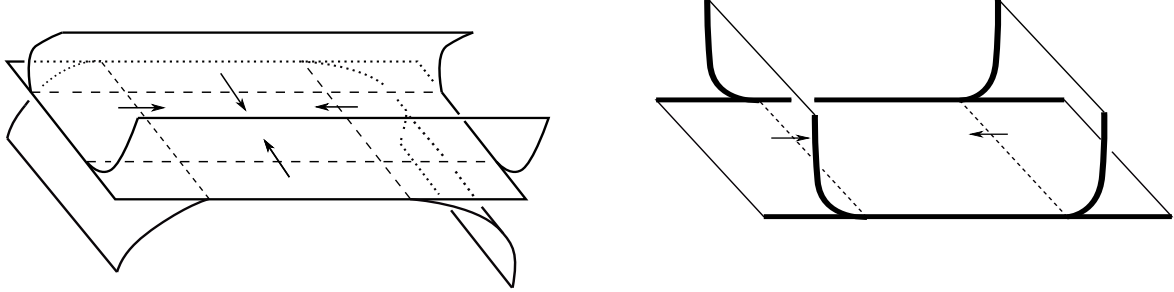


FIGURE 3. On the left, the local model of a **sink disk**. On the right, the **bolded** lines lie on $\partial M \approx T^2$; this is the local model for a **half sink disk**.

Gabai and Oertel prove a lamination \mathcal{L} is essential if and only if \mathcal{L} is carried by an essential branched surface B [GO89]. Li proves that for B to carry an essential lamination, it must be sink disk free:

Theorem 2.4 (Theorem 2.5 in [Li03]). *Suppose M is an irreducible and orientable 3-manifold whose boundary is an incompressible torus, and B is a properly embedded branched surface in M such that*

- (1a) $\partial_h(N(B))$ is incompressible and ∂ -incompressible in $M - \text{int}(N(B))$
- (1b) There is no monogon in $M - \text{int}(N(B))$
- (1c) No component of $\partial_h N(B)$ is a sphere or a disk properly embedded in M
- (2) $M - \text{int}(N(B))$ is irreducible and $\partial M - \text{int}(N(B))$ is incompressible in $M - \text{int}(N(B))$
- (3) B contains no Reeb branched surface (see [GO89] for more details)
- (4) B is sink disk free

Suppose r is any slope in $\mathbb{Q} \cup \{\infty\}$ realized by the boundary train track $\tau_B = B \cap \partial X_K$. If B does not carry a torus that bounds a solid torus in $M(r)$, the manifold obtained by r -framed Dehn filling, then (1) B carries an essential lamination in M meeting the boundary torus in parallel simple closed curves of slope r , and (2) $M(r)$ contains an essential lamination.

Remark 2.5. Our version of Theorem 2.4 differs mildly from the version in [Li03]. The discrepancy arises from our consideration of the lamination in M ; this is not problematic, as the lamination in $M(r)$ meets the surgery torus in simple closed curves of slope r .

A branched surface satisfying conditions (1–4) in Theorem 2.4 is called a **laminar branched surface**. To prove Theorem 1.2 for any positive 3-braid knot K , we construct a laminar branched surface B and prove the boundary train track τ carries all rational slopes $r < 2g(K) - 1$. Applying Theorem 2.4, we deduce the existence of essential laminations in X_K , which we extend to taut foliations in X_K .

2.2. Product Disks. Positive braid closures are fibered links [Sta78]. This statement can be proved concretely via disk decomposition [Gab86]. We recount the relevant details of Gabai's method.

For $K \subset S^3$, let F be a genus g orientable Seifert surface for K . $F \times I$ is a genus $2g$ handlebody H , and $\partial H \approx F^+ \cup F^- \cup A$, where $A \approx K \times I$. This is an example of a **sutured manifold** with annular suture A , formally written as $(F \times I, \partial F \times I) \approx (F \times I, K \times I) \approx (M, \gamma)$.

A **product disk** is a disk D^2 in the **complementary sutured manifold** $(X_F, \partial F \times I)$, $X_F := \overline{S^3 - (F \times I)}$, such that $\partial D^2 \approx S^1$ meets the suture A exactly twice. Given a product disk in X_F , we can **decompose along it**, by cutting X_F along D and creating a new sutured manifold $M' \approx \overline{X_F - (D \times I)}$. The sutures γ of M can be modified in one of two ways to form the sutures γ' of M' : at the sites where $\gamma \cap \partial M'$, connect the ends of $\gamma \cap (\partial D \times \{\pm 1\})$ by diameters of $D \times \{\pm 1\}$. Writing $(M, \gamma) \xrightarrow{D} (M', \gamma')$ denotes a **(product) disk decomposition**.

Theorem 2.6 (Theorem 1.9 in [Gab86]). *A link $L \subset S^3$ is fibered with fiber surface F if and only if a sequence of product disk decompositions, applied to $(X_F, \partial F \times I)$, terminates with a collection of product sutured balls $(B^3, S^1 \times I)$.*

When K is a fibered knot in S^3 , the sequence of product disk decompositions terminates with a single $(B^3, S^1 \times I)$.

A sequence of disk decompositions to a product sutured ball not only certifies fiberedness, but also determines where the monodromy sends properly embedded arcs on F . Let F be a fiber surface for $K \subset S^3$, and let α be an essential properly embedded arc on F^- . View α as an arc on $F^- \subset \partial(F \times I)$ with $\partial\alpha \subset \partial A$. $(F \times I, A)$ is a trivial product sutured manifold; heuristically, all the data pertaining to the monodromy of the fibered knot is captured by the complementary sutured manifold. In particular, pushing α through the $(X_F, \partial F \times I)$ yields a disk D , where ∂D meets the suture twice, and $\partial D - A = \alpha^+ \sqcup \alpha^-$, where $\alpha^* \subset F^*$. D is a product disk, and $\varphi(\alpha^-) \approx \alpha^+$.

Remark 2.7. *Positive braid closures are obtained by a sequence of plumbings of positive Hopf bands. One can inductively apply Corollary 1.4 in [Gab85] to produce an explicit factorization of the monodromy in terms of Dehn twists.*

2.3. Constructing the Fiber Surface for Positive 3-braid Closures: Up to conjugation and applications of the braid relation $\sigma_1\sigma_2\sigma_1 = \sigma_2\sigma_1\sigma_2$, every positive 3-braid can be written in the form

$$(2.1) \quad \beta = \sigma_1^{a_1} \sigma_2^{b_1} \sigma_1^{a_2} \sigma_2^{b_2} \dots \sigma_1^{a_k} \sigma_2^{b_k}$$

with $a_i \geq 2, b_i \geq 1$ for all $1 \leq i \leq k$. Going forward, we assume all 3-braids are in this form.

Definition 2.8. *Let β be of the form described in (2.1). β has k **blocks**, where the i^{th} block has the form $\sigma_1^{a_i} \sigma_2^{b_i}$.*

Definition 2.9. Let $\hat{\beta}$ denote the closure of β , which is in the form specified by Equation 2.1. Define:

$$c_1 := \sum_{i=1}^k a_i \quad c_2 := \sum_{i=1}^k b_i$$

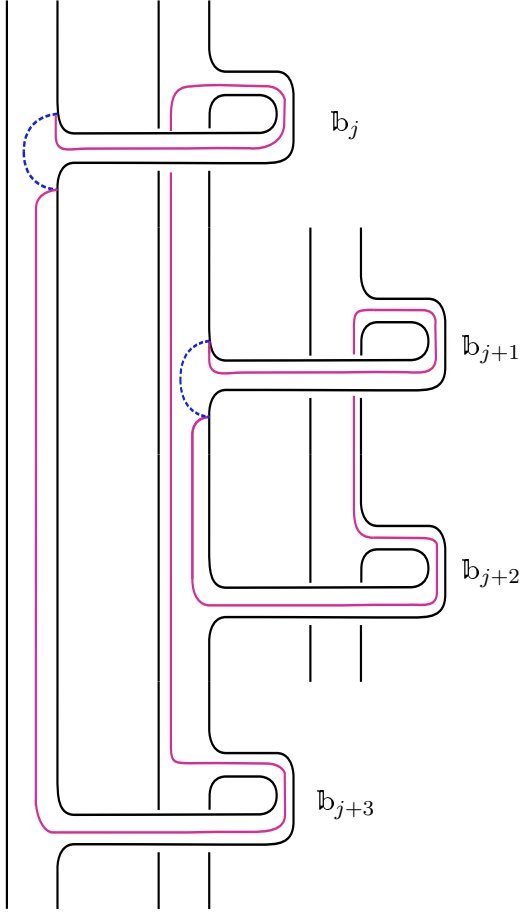


FIGURE 4. There are two product disks identified, D_j and D_{j+1} . $\partial D_j \subset S_1 \cup S_2 \cup \mathbb{b}_j \cup \mathbb{b}_{j+3}$, and $\partial D_{j+1} \subset S_2 \cup S_3 \cup \mathbb{b}_{j+1} \cup \mathbb{b}_{j+2}$.

Applying Seifert's algorithm to $\hat{\beta}$ yields Seifert disks S_1, S_2, S_3 . Reading β from left to right, each occurrence of σ_i dictates the attachment of a positively twisted band between S_i and S_{i+1} .

Definition 2.10. For the j^{th} letter σ_i in the braid word β , denote the corresponding positively twisted band attached between S_i and S_{i+1} as \mathbb{b}_j .

The bands are attached from top to bottom; there are $c_1 + c_2$ bands attached in total. This is our fiber surface F for $\hat{\beta}$. Following conventions established by Rudolph [Rud93], we only see F^+ , the “positive side” of F , in our figures.

Definition 2.11. The bands \mathbb{b}_j and \mathbb{b}_k are **of the same type** if they are both attached between the Seifert disks S_i and S_{i+1} .

It is straightforward to identify a collection of product disks for F : the boundary of a disk D_j will be entirely contained in $\mathbb{b}_j, \mathbb{b}_k$ (the next band of the same type as \mathbb{b}_j), and $S_i \cup S_{i+1} \cup A$ (where S_i and S_{i+1} are the Seifert disks to which \mathbb{b}_j and \mathbb{b}_k are attached). Decomposing X_F along $c_1 + c_2 - 2$ disks results in a single product sutured ball. Since fiber surfaces are minimal genus Seifert surfaces, we conclude $\chi(F) = 3 - (c_1 + c_2)$ and $2g(K) - 1 = c_1 + c_2 - 3$.

Definition 2.12. Suppose a product disk has boundary contained in \mathbb{b}_j and \mathbb{b}_k , which are bands of the same type with $j < k$. We refer to this disk as D_j . Furthermore, we denote the non-sutured portion of $\partial D_j, \overline{\partial D_j - A}$, by $\alpha_j^+ \cup \alpha_j^-$, where $\alpha_j^* \subset F^*$.

The product disk D_j is completely determined by the arcs α_j^- and $\alpha_j^+ \approx \varphi(\alpha_j^-)$. As in Figure 4, we draw α_j^\pm on $F \times \{\frac{1}{2}\}$, not in $(X_F, K \times I)$.

3. FOUNDATIONS FOR THEOREM 1.2

This section provides the structure of proof of Theorem 1.2 and a series of important lemmas towards that end. We establish notation for constructing and analyzing branched surfaces in exteriors of positive 3-braid closures. The proof of Theorem 1.2, in Section 4, requires analysis of 3 cases; we carry out the example of $P(-2, 3, 7)$ here alongside our preparatory material as motivation. This example already contains the richness of the several cases required to prove Theorem 1.2.

We outline the construction of taut foliations in $S_r^3(K)$, K realized as the closure of a positive 3-braid, $r \in (-\infty, 2g(K) - 1)$:

- Section 3.1:* Identify $c_1 + c_2 - 2$ disjoint product disks $\{D_j\}$ in X_F
- Section 3.2:* Isotope $\{D_j\}$ into a standardized position in X_K
- Section 3.3:* Build the spine of the branched surface in X_K from a copy of the fiber surface F and these standardized disks
- Section 3.4:* Build the laminar branched surface B :
 - Section 3.4.1:* Assign optimal co-orientations for the standardized $\{D_j\}$
 - Section 3.4.2:* Check B is sink disk free
 - Section 3.4.3:* Prove B is a laminar branched surface
- Section 3.5:* Construct taut foliations in X_K :
 - Section 3.5.1:* Show the boundary train track τ carries all slopes $(-\infty, 2g(K) - 1)$
 - Section 3.5.2:* Extend essential laminations to taut foliations in X_K
 - Section 3.5.3:* Produce taut foliations in $S_r^3(K)$ via Dehn filling

To begin our motivational example, we note that $P(-2, 3, 7)$ is the closure of a positive 3-braid. In particular, $P(-2, 3, 7) = \hat{\beta}$, for $\beta = \sigma_1^7 \sigma_2^2 \sigma_1^2 \sigma_2$.

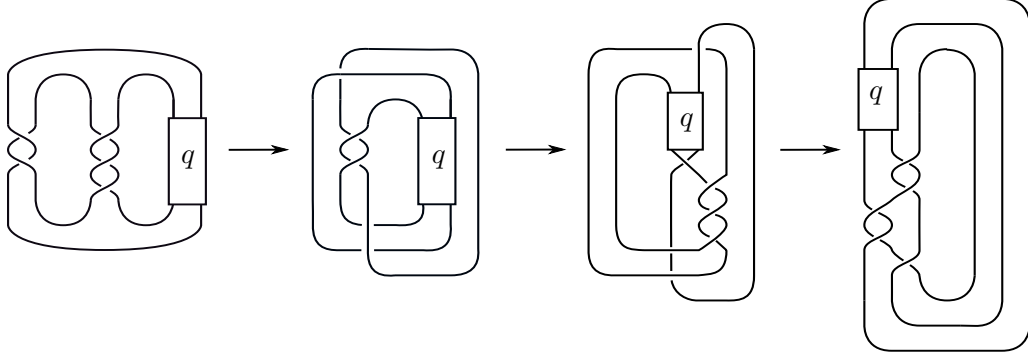


FIGURE 5. An isotopy of $P(-2, 3, q)$, q odd, $q \geq 1$ into the positive closed 3-braid $\hat{\beta}$, for $\beta = \sigma_1^q \sigma_2^2 \sigma_1^2 \sigma_2$.

3.1. Identify disjoint product disks $\{D_j\}$ in X_F . The setup in Section 2.3 supplies $c_1 + c_2 - 2$ product disks: take the product disks used to show F is a fiber surface for K .

Figure 6 shows the fiber surface for $P(-2, 3, 7)$, and 10 product disks $\{D_1, \dots, D_{10}\}$. The disks $\{D_1, D_2, \dots, D_7, D_{10}\}$ have boundaries contained in $\mathbb{b}_1 \cup \dots \cup \mathbb{b}_7 \cup \mathbb{b}_{10} \cup \mathbb{b}_{11} \cup S_1 \cup S_2$;

the disks $\{D_8, D_9\}$ have boundaries contained in $\mathbb{b}_8 \cup \mathbb{b}_9 \cup \mathbb{b}_{12} \cup S_2 \cup S_3$. The product disks D_1, \dots, D_{10} are disjoint in X_F , as $\alpha_1^-, \dots, \alpha_{10}^-$ are pairwise disjoint.

3.2. Isotope $\{D_j\}$ into a standardized position in X_K . The $c_1 + c_2 - 2$ product disks found in Section 3.1 are contained in the surface exterior $X_F \approx \overline{X_K - (F \times [\frac{1}{4}, \frac{3}{4}])}$. Collapsing $F \times [\frac{1}{4}, \frac{3}{4}]$ to $F \times \{\frac{1}{2}\}$ produces $c_1 + c_2 - 2$ disks in X_K , with $\partial D_j \subset (F \times \{1/2\}) \cup \partial X_K$.

Consider $(F \times \{\frac{1}{2}\}) \cup (D_1 \cup \dots \cup D_{c_1+c_2-2})$ in X_K . This is the spine for a branched surface in X_K . For all $j \neq \ell$ and fixed $\star \in \{+, -\}$, the arcs α_j^\star and α_ℓ^\star are disjoint on the fiber surface $F \times \{\frac{1}{2}\}$. However, for $j \neq \ell$, it is possible for α_j^+ and α_ℓ^- to intersect on $F \times \{\frac{1}{2}\}$; after smoothing, there will be many triple points, as in Figure 2.

We want to simplify the forthcoming branched surface. To this end, we isotope the product disks $D_1, \dots, D_{c_1+c_2-2}$ in X_K such that the arcs $\{\alpha_j^\pm\}$ intersect minimally on $F \times \{\frac{1}{2}\}$.

There are two types of intersection points between α_j^+ and α_ℓ^- , $j \neq \ell$:

Definition 3.1. A **Type 1 intersection point** arises from $\alpha_j^+ \cap \alpha_{j+1}^-$, where \mathbb{b}_j and \mathbb{b}_{j+1} are bands of the same type. A **Type 2 intersection point** arises from $\alpha_j^+ \cap \alpha_\ell^-$, where \mathbb{b}_j and \mathbb{b}_ℓ are bands associated to the last occurrences of σ_1 and σ_2 in the same block $\sigma_1^{a_i} \sigma_2^{b_i}$.

In Figure 6, we see nine triple points in the spine of $P(-2, 3, 7)$: there are eight Type 1 intersection points, and a single Type 2 intersection point. Lemma 3.4 will eliminate all Type 1 intersection points.

Definition 3.2. Let D_j be a product disk in the spine of a branched surface. A **spinal isotopy** $\iota_j : D_j \times [0, 1] \rightarrow X_K$ is an isotopy of the disk D_j in X_K such that for all $t \in [0, 1]$,

- $\iota_j|_{\alpha_j^- \times \{t\}} = \mathbb{1}$
- $\iota_j(\alpha_j^+ \times \{t\}) \subset (F \times \{\frac{1}{2}\})^+$
- $(\partial D \cap \partial X_K) \subset \partial X_K$
- $\mathring{D} \subset X_K - (F \times \{\frac{1}{2}\})$

and $\iota_j(\alpha_j^+ \times \{1\}) \subset S_i$, where $i = 2, 3$.

Intuitively, allowing α_j^+ to move freely along $F \times \{\frac{1}{2}\}$ guides an isotopy of D_j in X_K .

Definition 3.3. An arc α_j^+ is in **standard position** if it has been isotoped to lie entirely in a single Seifert disk S_i , $i = 2, 3$. A disk is in **standard position** if both α_j^+ and α_j^- lie entirely in $S_1 \cup S_2 \cup S_3$.

Lemma 3.4. There exists a sequence of $c_1 + c_2 - 2$ spinal isotopies of the disks $D_1, \dots, D_{c_1+c_2-2}$ putting all disks in standard position. Equivalently, there exists a splitting of the spine of the branched surface with no Type 1 intersection points, i.e. with $\alpha_1^+, \dots, \alpha_{c_1+c_2-2}^+$ in standard position.

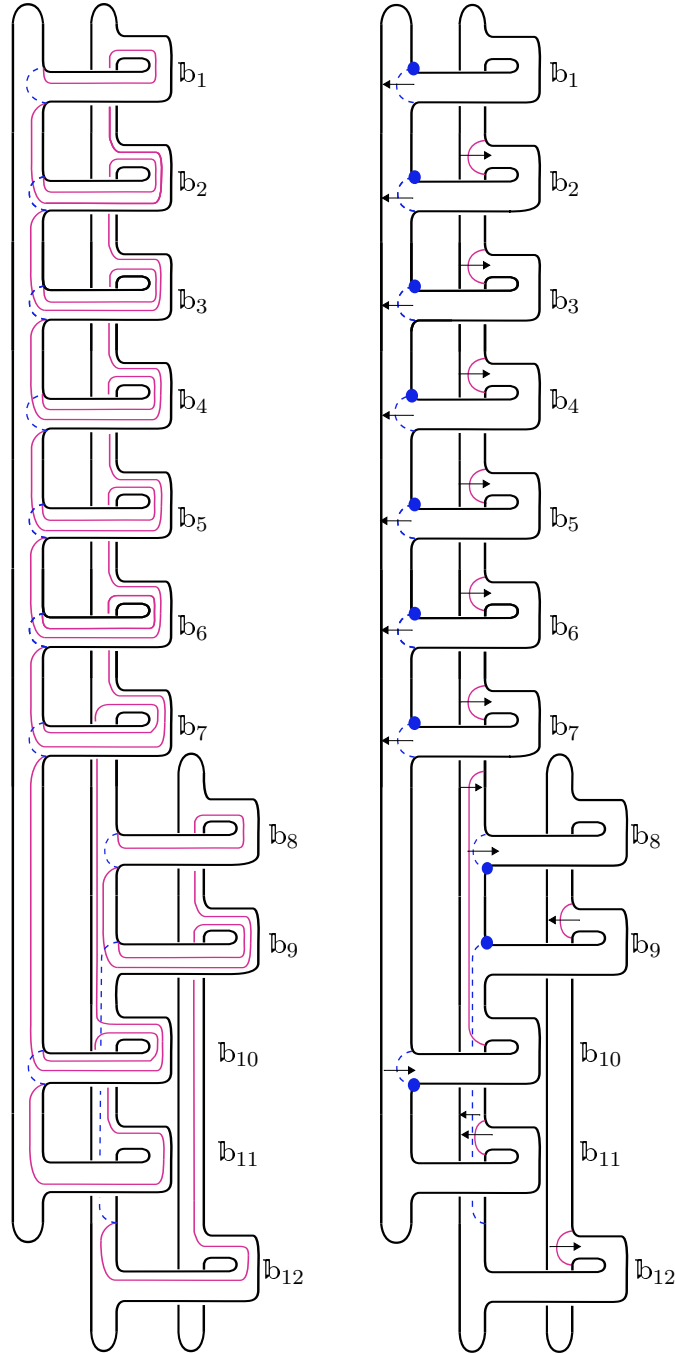


FIGURE 6. On the left: the fiber surface and 10 product disks for $P(-2, 3, 7)$. On the right: the lamina branched surface for $P(-2, 3, 7)$ with cusping directions $(\leftarrow)^7(\rightarrow)(\leftarrow)(\rightarrow)(\leftarrow)(\leftarrow)$.

Proof. Scanning the diagram of $F \times \{\frac{1}{2}\}$ from bottom to top, find the first arc α_s^+ encountered. The last letter of β is σ_2 , so $\alpha_s^+ \subset \mathbb{b}_s \cup \mathbb{b}_{c_1+c_2} \cup S_2 \cup S_3$, with $s < c_1 + c_2$. If we allow *free* isotopy of arcs in $F \times \frac{1}{2}$ (i.e. an isotopy i_s of α_s^+ where the endpoints of the arc can move along ∂F), α_s^+ can be isotoped to lie entirely in S_3 . Let ι_s be the spinal isotopy of D_s in X_K such that for all t , $\iota_s(\alpha_s^+ \times \{t\}) = i_s(\alpha_s^+ \times \{t\})$. Applying ι_s puts D_s in standard position.

Continue scanning the diagram from bottom to top, and find the next arc α_r^+ encountered. Apply the spinal isotopy ι_r of D_r in X_K such that $\iota_r|_{\alpha_r^+ \times \{t\}}$ pushes α_r^+ into standard position. After $c_1 + c_2 - 2$ iterations of this procedure (finding the next arc α_m^+ encountered, and putting the disk D_m in standard position via ι_m), all disks are standardized. A Type 1 intersection between α_t^+ and α_{t+1}^- is eliminated by the isotopy ι_t standardizing D_t . \square

Remark 3.5. *The pre- and post-split spine have isotopic exteriors.*

For $P(-2, 3, 7)$, the arcs get isotoped in the following order:

$$\alpha_9^+, \alpha_{10}^+, \alpha_7^+, \alpha_8^+, \alpha_6^+, \alpha_5^+, \alpha_4^+, \alpha_3^+, \alpha_2^+, \alpha_1^+$$

The result of applying Lemma 3.4 is seen in the right diagram in Figure 6. There is a single Type 2 intersection point between α_7^+ and α_9^- .

Going forward, all disks D_j are in standard position, unless stated otherwise. We will **not** change our notation to indicate the disks are standardized.

3.3. Build the spine of the branched surface. The spine for the branched surface is built from

$$(F \times \{1/2\}) \cup \left(\bigcup_{i=1}^{c_1+c_2-2} D_i \right)$$

For $P(-2, 3, 7)$, the spine for the branched surface is in Figure 6.

3.4. Build the branched surface B . To build the laminar branched surface, we need to assign co-orientations for the disks D_j , $1 \leq j \leq c_1 + c_2 - 2$, and verify these choices do not create sink disks. To achieve these goals, we study the branch locus and branch sectors.

Lemma 3.4 simplified the branch locus: all arcs α_j^\pm , $1 \leq j \leq c_1 + c_2 - 2$ are now contained in $S_1 \cup S_2 \cup S_3$. Moreover, arcs α_j^- are isotopic to the co-cores of bands \mathbb{b}_j , or would be if other bands were not obstructing the path of the lower endpoint.

For $P(-2, 3, 7)$,

- the arcs $\alpha_1^-, \dots, \alpha_7^-, \alpha_{10}^-$, contained in S_1 , are isotopic to the co-cores of the 1-handles $\mathbb{b}_1, \dots, \mathbb{b}_7, \mathbb{b}_{10}$ respectively.
- the arc α_8^- is isotopic to the co-core of \mathbb{b}_8 .
- the arcs $\alpha_1^+, \dots, \alpha_6^+, \alpha_{10}^+$ are isotopic to the co-cores of the 1-handles $\mathbb{b}_2, \dots, \mathbb{b}_7, \mathbb{b}_{11}$, respectively, and are contained in S_2 .
- the α_8^+ is isotopic to the co-core of \mathbb{b}_9 , and is contained in S_3 .
- the two arcs α_9^- and α_7^+ are not isotopic to the co-cores of any bands.

Cusp directions for the disks have yet to be assigned. Nevertheless, we know the branch sectors for B will fall into two categories: the sectors that lie in $F \times \{\frac{1}{2}\}$, and sectors arising from isotoped product disks. The former can be further refined into 3 categories:

Definition 3.6. *The S_i **disk sector** is the connected component of a branch sector containing the Seifert disk S_i . A **band sector** is the connected component of a branch sector associated to a positively twisted band. The remaining branch sectors are **polygon sectors**; each lies in a single Seifert disk.*

In particular, all polygon sectors lie in S_2 . For $P(-2, 3, 7)$, there are 7 band sectors (the branch sectors containing $\mathbb{b}_2, \dots, \mathbb{b}_7 \cup \mathbb{b}_9 \cup \mathbb{b}_{10}$), and a pair of polygon sectors.

3.4.1. Assign optimal co-orientations to $\{D_j\}$.

Definition 3.7. *Let $\hat{\alpha}_j^\star$ denote the cusp direction of α_j^\star , for $\star \in \{+, -\}$.*

Lemma 3.8. *Assigning a co-orientation to D_j determines the cusp orientation to both α_j^+ and α_j^- . Moreover, if we orient the arcs α_j^\pm from the lower endpoint to the upper endpoint, the pairings $\langle \alpha_j^+, \hat{\alpha}_j^+ \rangle$ and $\langle \alpha_j^-, \hat{\alpha}_j^- \rangle$ have opposite signs.*

Heuristically: the induced cusp orientations of α_j^+ and α_j^- “point in opposite directions” when looking at $(F \times \{\frac{1}{2}\})^+$.

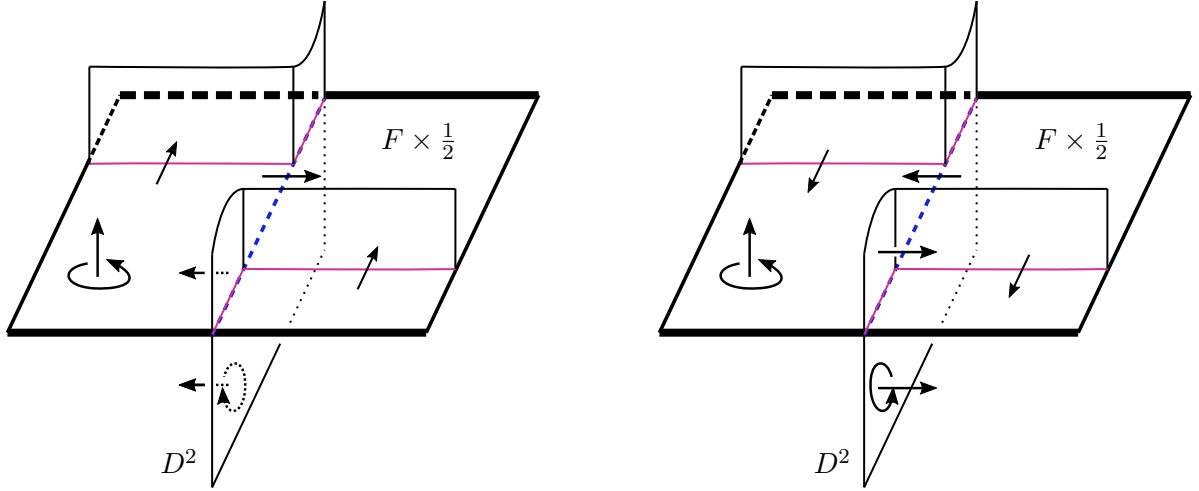


FIGURE 7. In this local model, we have fixed a co-orientation on $F \times \{\frac{1}{2}\}$, and chosen different co-orientations on D_j in the left and right figures. The correct cusping choices for α_j^\pm are provided. The **bolded** horizontal lines lie on ∂X_K .

Proof. For simplicity, assume the disk has yet to be standardized. Choose a co-orientation on D_j . Since F is co-oriented, the correct smoothing choices for α_j^+ and α_j^- ensure the co-orientations of F and D_j agree near the branch locus. The corresponding cusp directions for

α_j^\pm can be determined immediately, as in the local model in Figure 7: if the cusp direction on α_j^- points to the right (resp. left) near ∂X_K , then the cusp direction on α_j^+ points to the left (resp. right) near ∂X_K . Taking a global viewpoint as in Figure 8, orient the arcs α_j^\pm from the lower endpoint to the upper endpoint: the pairings $\langle \alpha_j^\pm, \hat{\alpha}_j^\pm \rangle$ have opposite signs, and the cusp directions point in opposite directions when looking at $(F \times \{\frac{1}{2}\})^+$. Our isotopy ι_t of D_t preserves the relative positions of the upper and lower endpoints of α_t^+ , so the lemma holds for standardized disks. \square

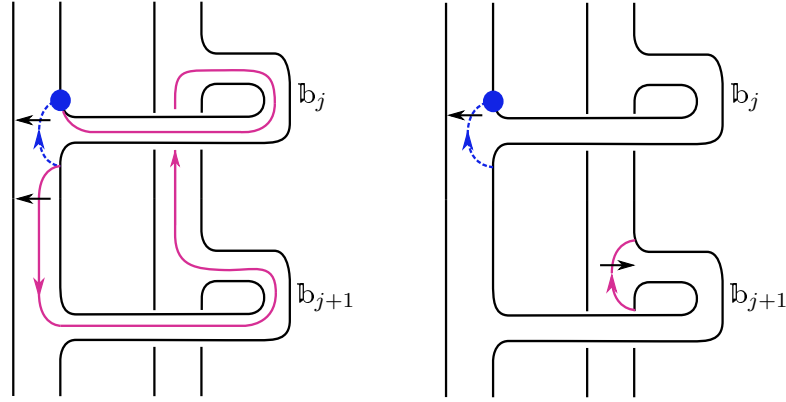


FIGURE 8. After standardizing, $\hat{\alpha}_j^-$ and $\hat{\alpha}_j^+$ “point in opposite directions”.

The cusp direction of α_j^- determines the co-orientation of D_j . Moreover, the upper endpoint of α_j^- is planted above the attachment site of the 1-handle \mathbb{b}_j , which in turn is associated to the j^{th} letter σ_i of β . Therefore, we can encode the co-orientation of D_j directly to \mathbb{b}_j , via the induced cusp orientation on α_j^- .

Definition 3.9. We encode the co-orientation of D_j by recording the cusp direction of α_i^- in tandem with β . For σ the j^{th} letter of β :

- Writing \leftarrow below σ indicates $\langle \hat{\alpha}_j^-, \alpha_j^- \rangle = 1$ and $\langle \hat{\alpha}_j^+, \alpha_j^+ \rangle = -1$. That is, α_j^- is cusped “to the left”, and α_j^+ is cusped “to the right” when looking at $(F \times \{\frac{1}{2}\})^+$.
- Writing \rightarrow below σ indicates $\langle \hat{\alpha}_j^-, \alpha_j^- \rangle = -1$ and $\langle \hat{\alpha}_j^+, \alpha_j^+ \rangle = 1$. That is, α_j^- is cusped “to the right”, and α_j^+ is cusped “to the left” when looking at $(F \times \{\frac{1}{2}\})^+$.
- Writing $()$ below σ indicates **not** choosing the product disk D_j with pre-standardized arc α_j^+ passing through this 1-handle. We say σ is **uncusped**.

$P(-2, 3, 7)$ is realized as the closure of $\beta = \sigma_1^7 \sigma_2^2 \sigma_1^2 \sigma_2 = \sigma_1^7 \sigma_2 \sigma_2 \sigma_1 \sigma_1 \sigma_2$. The cusping directions in (3.1) below determine a branched surface – it specifies which product disks to choose when building the spine, and how to co-orient them, as in Figure 6.

$$(3.1) \quad \begin{array}{ccccccc} \sigma_1^7 & \sigma_2 & \sigma_2 & \sigma_1 & \sigma_1 & \sigma_2 & \\ (\leftarrow)^7 (\rightarrow) (\leftarrow) (\rightarrow) () () \end{array}$$

We emphasize: directions, as in (3.1), completely determine a branched surface. In Section 4.2, we assign cusp directions for an arbitrary positive 3-braid closure.

3.4.2. Check B is sink disk free.

Lemma 3.10. *A branch sector arising from an isotoped product disk is never a sink disk.*

Proof. Let D_j be any product disk sector. By Lemma 3.8, the pairings $\langle \alpha_j^+, \hat{\alpha}_j^+ \rangle$ and $\langle \alpha_j^-, \hat{\alpha}_j^- \rangle$ have opposite signs. Therefore, one of $\hat{\alpha}_j^+$ and $\hat{\alpha}_j^-$ points out of $(F \times \{\frac{1}{2}\})^+$ and into D_j (and vice-versa for the other). It is impossible for both cusp directions to point into D_j . \square

In Section 4, we develop techniques for determining which cusping directions (as in (3.1)) create sink disks. For the branched surface B for $P(-2, 3, 7)$, we already identified the branch sectors on $F \times \{\frac{1}{2}\}$, so verifying B is sink disk free is straightforward. To show a branch sector is not a half sink disk, we need only check some cusped arc $\hat{\alpha}_j^*$ points out of it.

- The Disk Sectors
 - S_1 is not a sink disk, because $\hat{\alpha}_{10}^-$ points out of it.
 - S_2 is not a sink disk, because $\hat{\alpha}_1^+$ points out of it.
 - S_3 is not a sink disk, because $\hat{\alpha}_9^+$ points out of it.
- The Band Sectors
 - The sectors $\mathbb{b}_2, \dots, \mathbb{b}_7$ have $\hat{\alpha}_2^-, \dots, \hat{\alpha}_7^-$ pointing out of the respective regions.
 - The band sector containing $\mathbb{b}_9 \cup \mathbb{b}_{10}$ in the boundary has $\hat{\alpha}_9^-$ pointing out of it.
- The Polygon Sectors
 - The boundary of the **upper polygon sector** P_u is contained in $\alpha_7^+ \cup \alpha_8^- \cup \alpha_9^- \cup \partial F$; $\hat{\alpha}_8^-$ points out of the sector.
 - The boundary of the **lower polygon sector** P_ℓ is contained in $\alpha_7^+ \cup \alpha_9^- \cup \alpha_{10}^+ \cup \partial F$; $\hat{\alpha}_9^-$ points out of the sector.

3.4.3. B is a laminar branched surface.

Proposition 3.11. *A sink disk free branched surface B , constructed from a copy of the fiber surface and a collection of product disks, is a laminar branched surface.*

Proof. We verify B is laminar by verifying conditions (1) – (4) of Theorem 2.4 hold. Note that the M of Theorem 2.4 is X_K .

(1a) $\partial_h(N(B))$ is incompressible and ∂ -incompressible in $M - \text{int}(N(B))$.

A sutured manifold (M, γ) is **taut** if M is irreducible and $R(\gamma)$ is norm minimizing in $H_2(M, \gamma)$ [Gab83]. Each of our product disks appears in a sutured manifold decomposition of $(X_F, K \times I)$ which terminates in $(D^2, S^1 \times I)$. Thus, any sutured manifold appearing in the sequence of product disk decompositions of $(X_F, K \times I)$ is a taut sutured manifold [Gab83]. In particular, the exterior of the pre-split spine (built from $c_1 + c_2 - 2$ co-oriented product disks), (M', γ'_M) , is a taut product sutured manifold, and $R(\gamma'_M)$ is norm minimizing.

The exterior of the post-split spine also has a product sutured manifold structure; denote this manifold (N', γ'_N) . For B the branched surface whose spine has standardized disks, we have $\gamma'_N \approx \partial_v(N(B)) \cup (\partial X_K - \text{int}(N(B))|_{\partial X_K})$ and $R(\gamma'_N)$ is isotopic to $R(\gamma'_M) \approx \partial_h(N(B))$. Thus $\partial_h N(B)$ is norm minimizing in $H_2(N', \gamma'_N)$, and $\partial_h(N(B))$ is incompressible and ∂ -incompressible in $M - \text{int}(N(B))$.

- (1b) **There is no monogon in $M - \text{int}(N(B))$.**

This follows from our construction.

- (1c) **No component of $\partial_h N(B)$ is a sphere or a disk properly embedded in M .**

Every component of $\partial_h N(B)$ meets ∂X_K , so no component of $\partial_h(N(B))$ can be a sphere. The horizontal boundary $\partial_h N(B)$ is properly embedded in X_B , not X_K .

- (2) **$M - \text{int}(N(B))$ is irreducible and $\partial M - \text{int}(N(B))$ is incompressible in $M - \text{int}(N(B))$.**

$M - \text{int}(N(B))$ is a submanifold of S^3 , thus is irreducible. $\partial X_K - \text{int}(N(B))$ is a torus with a neighborhood of a train track removed: it is a collection of bigons. In particular, any simple closed curve in $\partial X_K - \text{int}(N(B))$ bounds a disk in $\partial X_K - \text{int}(N(B))$, and is incompressible in $M - \text{int}(N(B))$.

- (3) **B contains no Reeb branched surface (see [GO89] for more details).**

B is properly embedded in X_K , so any surface carried by B must also be properly embedded in X_K . Thus B cannot carry a torus, and B contains no Reeb branched surface.

- (4) **B is sink disk free.**

This holds by assumption. □

3.5. Construct taut foliations in X_K . B is a laminar branched surface. Theorem 2.4 guarantees that for every rational slope r carried by the boundary train track τ , there exists an essential lamination \mathcal{L}_r meeting ∂X_K in simple closed curves of slope r . To construct taut foliations in X_K , we first understand which slopes are carried by τ , apply Theorem 2.4 to get a family of essential laminations, and then extend each lamination to a taut foliation in X_K .

3.5.1. Show the train track τ carries all rational slopes $r < 2g(K) - 1$. Since B is formed by $(F \times \{\frac{1}{2}\}) \cup D_1 \cup \dots \cup D_{c_1+c_2-2}$, the boundary train track τ carries slope 0.

Definition 3.12. *Each D_j meets ∂X_K in two arcs, each tracing out the path of an endpoint of α_j^- under φ . These arcs are **sectors of the train track** τ ; $\overline{\tau - \lambda}$ is a collection of sectors.*

We have $c_1 + c_2 - 2$ disks, and therefore $2 \cdot (c_1 + c_2 - 2)$ sectors in the associated train track τ . Consider α_j^- with cusping $\widehat{\alpha}_j^-$. The cusping $\widehat{\alpha}_j^-$ will agree with the orientation of λ at one endpoint of α_j^- , and disagree at the other endpoint. Thus, for s_j and s'_j the pair of sectors induced by α_j^- , the train tracks $\lambda \cup s_j$ and $\lambda \cup s'_j$ carry different slopes, as in Figure 9: $\lambda \cup$ (the leftmost sector) carries $[0, 1)$, while $\lambda \cup$ (the middle sector) carries $(-\infty, 0]$.

Definition 3.13. *If the direction of $\widehat{\alpha}_j^-$ disagrees with the orientation of λ at a given endpoint of α_j^- , we say this endpoint **contributes maximally** to τ .*

In our figures, the endpoint of α_j^- contributing maximally is **bolded**.

Our goal is to maximize the interval of slopes carried by τ . There are $c_1 + c_2 - 2$ endpoints contributing maximally to τ – one for each product disk. It is tempting to claim τ carries all slopes $[0, c_1 + c_2 - 2)$. However, this is naïve: the endpoints of the arcs α, α' could be linked on along ∂F , as in the rightmost picture in Figure 9.

Definition 3.14. *Let α_j^- and α_ℓ^- be distinct properly embedded arcs on F such that (1) the first endpoint of each arc contributes maximally to τ and (2) their endpoints are linked in λ . Then α_j^- and α_ℓ^- **linked arcs**. See Figure 9. If α_j^- and α_ℓ^- are not linked, they are **disjoint**.*

The train track τ induced by B will carry all slopes in $(-\infty, k)$, where k is the maximum number of pairwise disjoint arcs contributing maximally to τ . Proving Theorem 1.2 requires sorting positive 3-braids into three types. For each type, we construct a laminar branched surface B using $c_1 + c_2 - 2$ product disks and a unique pair of linked arcs. Thus, τ carries all slopes in $[0, (c_1 + c_2 - 2) - 1) = [0, 2g(K) - 1)$.

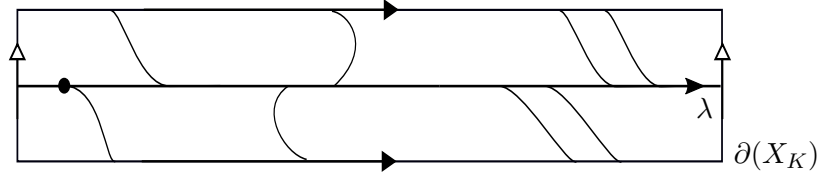


FIGURE 9. A train track $\tau \subset \partial(X_K)$. $\lambda \cup$ (the leftmost sector) carries $[0, 1)$, while $\lambda \cup$ (the middle sector) carries $(-\infty, 0]$. The rightmost sectors are linked.

Definition 3.15. *A **sub-train-track** τ' of τ is a train track carrying slope 0, such that $\{\text{sectors of } \tau'\} \subseteq \{\text{sectors of } \tau\}$.*

Remark 3.16. *For our purposes, τ' will include all sectors contributing maximally to τ , and a single sector s with $\lambda \cup s$ carrying $(-\infty, 0]$.*

Lemma 3.17. *Any slope carried by τ' , a sub-train-track of τ , is also carried by τ . □*

For $P(-2, 3, 7)$, we have $c_1 + c_2 - 2 = 10$ sectors contributing maximally to τ , and exactly one pair of linked arcs coming from α_8^- and α_9^- . Let τ' be the sub-train-track built from the endpoints of $\alpha_1^-, \dots, \alpha_{10}^-$ that contribute maximally to τ . Thus τ' carries all rational slopes in $[0, 9)$. Appending the upper endpoint of α_8^- to τ' ensures τ' carries all slopes in $(-\infty, 9)$. Applying Lemma 3.17, we conclude τ , the train track induced by B , carries slopes in $(-\infty, 9)$.

3.5.2. Extend essential laminations to taut foliations. We now have a laminar branched surface B carrying all rational slopes in $(-\infty, 2g(K) - 1)$. By Theorem 2.4, B carries an essential lamination \mathcal{L}_r for every rational $r \in (-\infty, 2g(K) - 1)$. We use these laminations to construct taut foliations in X_K .

Proposition 3.18. *Let \mathcal{L}_r be an essential lamination carried by our laminar branched surface B , such that \mathcal{L}_r meets ∂X_K in simple closed curves of slope r . Then \mathcal{L}_r can be extended to a taut foliation in X_K , which foliates ∂X_K in parallel simple closed curves of slope r .*

Proof. In Proposition 3.11, we proved the branched surface exterior $X_B \approx \overline{X_K - \text{int}(N(B))}$ is isotopic to a product sutured manifold. In particular, X_B has an I -bundle structure. $N(B)$ is an I -bundle over B , thus $\overline{N(B) - \mathcal{L}_r}$ has an I -bundle structure. Endowing the lamination exterior $X_{\mathcal{L}_r} \approx \overline{X_K - \mathcal{L}_r}$ with an I -bundle structure yields a foliation \mathcal{F}_r for X_K which is induced by \mathcal{L}_r .

\mathcal{L}_r meets ∂X_K in simple closed curves of slope r , so $\overline{X_{\mathcal{L}_r}}|_{\partial X_K}$ is an r -sloped annulus A_r . A_r is formed from $X_B|_{\partial X_K}$ and $\overline{N(B) - \mathcal{L}_r}|_{\partial X_K}$, which both have I -bundle structures. Simultaneously endowing X_B and $\overline{N(B) - \mathcal{L}_r}$ with an I -bundle structure (as above) foliates A_r by circles of slope r ; thus ∂X_K is foliated by simple closed curves of slope r . \square

3.5.3. Produce taut foliations in $S_r^3(K)$ via Dehn filling. For all rational $r < 2g(K) - 1$, X_K admits a taut foliation \mathcal{F}_r foliating ∂X_K in simple closed curves of slope r . Performing r -framed Dehn filling endows $S_r^3(K)$ with a taut foliation.

To summarize for $P(-2, 3, 7)$: we constructed a laminar branched surface $B \subset X_K$. The induced train track τ carries all rational slopes in $(-\infty, 2g(K) - 1) = (-\infty, 9)$. Applying Proposition 3.11, Theorem 2.4 and Proposition 3.18, we deduce X_K admits taut foliations meeting the boundary torus T in simple closed curves of slope $r \in (-\infty, 2g(K) - 1)$. Performing r -framed Dehn filling yields $S_r^3(K)$ endowed with a taut foliation. These manifolds are non-L-spaces; we have produced the taut foliations predicted by Conjecture 1.1.

4. PROOF OF THEOREM 1.2

In this section, we prove our main theorem:

Theorem 1.2. *Let K be a knot in S^3 , realized as the closure of a positive 3-braid. Then for every rational $r < 2g(K) - 1$, the knot exterior $X_K := S^3 - \mathring{\nu}(K)$ admits taut foliations meeting the boundary torus T in parallel simple closed curves of slope r . Hence the manifold obtained by r -framed Dehn filling, $S_r^3(K)$, admits a taut foliation.*

The proof requires generalizing the $P(-2, 3, 7)$ example of Section 3. In Section 4.1, we prove a few lemmas. Three families of branched surfaces are constructed in Section 4.2.

4.1. Co-orienting Arcs. Given an arbitrary positive 3-braid word β , we choose $c_1 + c_2 - 2$ product disks, as in Section 3.1. We need a strategy for assigning co-orientations. As in Section 3.4.1, we will provide cusp directions in tandem with β , and analyze which cusping directions produce sink disks and linked arc pairs. We aim to maximize the slopes carried by τ while ensuring B is sink disk free.

Lemma 4.1. *Suppose the subword $\sigma_i \sigma_i$ arises as the j^{th} and $j + 1^{\text{st}}$ letters in β . The cusping directions $(\leftarrow)^2$, $(\rightarrow)^2$, and $(\rightarrow \leftarrow)$ prevent the band sector \mathfrak{b}_{j+1} from being a half sink disk.*

Proof. As in Figures 10 and 12, α_j^+ is isotopic to the co-core of \mathbb{b}_{j+1} . If $\hat{\alpha}_j^- = (\rightarrow)$, then by Lemma 3.8, $\hat{\alpha}_j^+ = (\leftarrow)$, hence the directions $(\rightarrow)^2$ and $(\rightarrow \leftarrow)$ do not make \mathbb{b}_{j+1} a half sink disk. The cusping directions $(\leftarrow)^2$ have $\hat{\alpha}_{j+1}^-$ pointing out of \mathbb{b}_{j+1} . \square

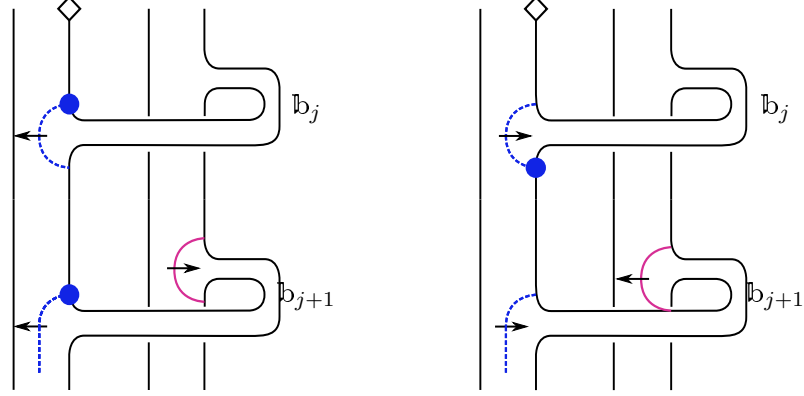


FIGURE 10. The directions $(\rightarrow)^2$ and $(\leftarrow)^2$ do not make \mathbb{b}_{j+1} a half sink disk.

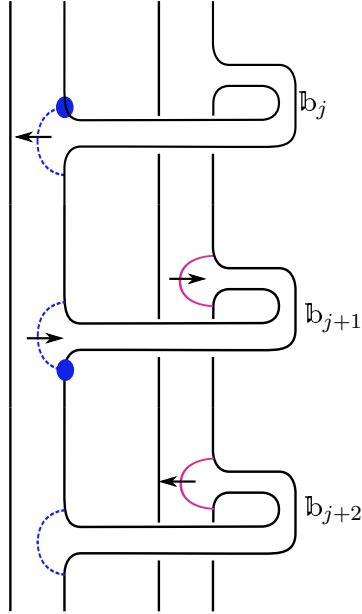


FIGURE 11. The band \mathbb{b}_{j+1} is a half sink disk.

Lemma 4.2. Suppose β contains the subword $\sigma_i \sigma_i \sigma_i$, arising as the $j, j+1, j+2$ letters of β . The cusping directions $(\leftarrow \rightarrow \star)$, $\star \in \{\rightarrow, \leftarrow, \quad\}$ force \mathbb{b}_{j+1} to be a half sink disk.

Proof. As in Figure 11, both α_{j+1}^- and α_j^+ are isotopic to the co-core of \mathbb{b}_{j+1} . Not only does $\widehat{\alpha}_{j+1}^-$ point into \mathbb{b}_{j+1} , but by Lemma 3.8, so does $\widehat{\alpha}_{j+1}^-$. \square

To produce a sink disk free branched surface, we should avoid the cusp directions $(\leftarrow \rightarrow)$.

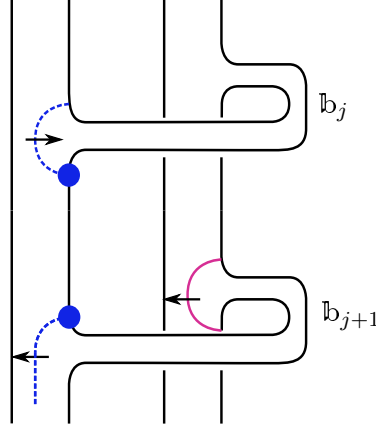


FIGURE 12. The arcs α_j^- and α_{j+1}^- are linked.

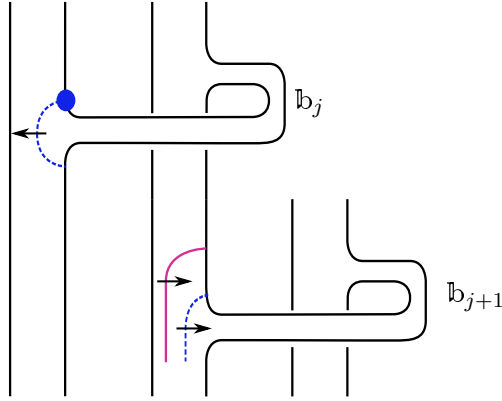


FIGURE 13. The arcs α_j^- and α_{j+1}^- are not linked.

Lemma 4.3. *Suppose β contains the subword $\sigma_i \sigma_i$ arising as the j^{th} and $j+1^{\text{st}}$ letters in the braid word β . The associated cusping directions $(\leftarrow \leftarrow)$ and $(\rightarrow \rightarrow)$ create an arc, disjoint from all other arcs, that contributes maximally to τ . The cusping directions $(\rightarrow \leftarrow)$ create a pair of linked arcs.*

Proof. First, suppose $(\sigma_i)^2$ is cusped via $(\leftarrow)^2$, as in the left picture in Figure 10. The bolded endpoints of α_j^- and α_{j+1}^- contribute maximally to τ . Traversing K from \diamond , we first encounter the upper endpoint of α_j^- , and then its image: no point that contributes maximally to τ

occurs between them. Thus α_j^- is disjoint from all other arcs. Analogously, if $(\sigma_i)^2$ is cusped via $(\rightarrow)^2$, α_j^- is disjoint from all other arcs, as in the right picture of Figure 10. If $(\sigma_i)^2$ is cusped via $(\rightarrow \leftarrow)$, α_j^- and α_{j+1}^- are linked, as in Figure 12. \square

Lemma 4.4. *Suppose the subword $\sigma_1\sigma_2$ occurs as the j and $j+1$ letters of β . The arcs α_j and α_{j+1} , cusped as $(\leftarrow \rightarrow)$, are disjoint.*

Proof. As in Figure 13, α_j^- is disjoint from α_{j+1} . \square

4.2. Building Branched Surfaces:

Definition 4.5. β has the form described in Equation 2.1. Then β is one of Types A, B, or C described below:

Type A: $k = 1$, and $\beta = \sigma_1^{a_1}\sigma_2^{b_1}$. For $\hat{\beta}$ to be a knot, a_1 and b_1 are both odd.

Note: $\hat{\beta} = T(2, a_1) \# T(2, b_1)$.

Type B: $k = 2$, and $b_1 = b_2 = 1$. So, $\beta = \sigma_1^{a_1}\sigma_2\sigma_1^{a_2}\sigma_2$

Type C: all other positive 3-braid closures; namely:

- $k = 2$ and (up to cyclic rotation) $a_1, a_2, b_1 \geq 2, b_2 \geq 1$
- $k \geq 3, a_i \geq 2, b_i \geq 1$ for all i .

Given a positive 3-braid knot, we construct a branched surface by fusing $c_1 + c_2 - 2$ product disks to $F \times \{\frac{1}{2}\}$, such that we have exactly one linked pair of arcs. Propositions 4.6, 4.7, 4.8 construct the branched surfaces for **Types A, B, and C** respectively.

Proposition 4.6. (Building the branched surface for **Type A**)

Suppose $\beta = \sigma_1^{a_1}\sigma_2^{b_1}$ for a_1, b_1 odd, and $K = \hat{\beta}$. There exists a sink-disk free branched surface $B \subset X_K$, for $K = T(2, a_1) \# T(2, b_1)$, with exactly one pair of linked arcs. Moreover, there exists a sub-train-track τ' of τ carrying all rational slopes $r < 2g(K) - 1$.

Proof. First suppose $a_1, b_1 \geq 3$. We identify $c_1 + c_2 - 2 = a_1 + b_1 - 2$ product disks:

$$(4.1) \quad \beta = \sigma_1^{a_1}\sigma_2^{b_1} = \sigma_1^{a_1-1} \quad \sigma_1 \quad \sigma_2^{b_1-2} \quad \sigma_2 \quad \sigma_2$$

$$(\rightarrow)^{a_1-1} \quad () \quad (\rightarrow)^{b_1-2} \quad (\leftarrow) \quad ()$$

The spine of the branched surface is built from $F \times \{\frac{1}{2}\}$, fused with the product disks specified. Applying Lemma 3.4 puts the product disks into standardized position; cusping as instructed in (4.1) yields a branched surface B . In this case, all arcs on $F \times \frac{1}{2}$ are pairwise disjoint (see Figure 14 for an example). Lemma 3.10 guarantees no product disk sector is a half sink disk, while Lemmas 4.1 and 4.2 guarantee no band sectors are half sink disks. There are no polygon sectors. We check the disk sectors S_1, S_2 , and S_3 are not half sink disks.

- $\hat{\alpha}_1^-$ points out of S_1 .
- $\hat{\alpha}_{a_1+1}^-$ points out of the S_2 disk sector.
- $\hat{\alpha}_{a_1+b_1-1}^-$ points into the S_2 disk sector, so $\hat{\alpha}_{a_1+b_1-1}^+$ points out of the S_3 disk sector.

B is sink disk free. By Lemma 4.3, $\alpha_{a_1+b_1-2}^-$ and $\alpha_{a_1+b_1-1}^-$ are the unique pair of linked arcs.

Now suppose $a_1 \geq 3$ and $b_1 = 1$, $a_1 = 1$ and $b_3 \geq 1$, or $a_1 = b_1 = 1$. Then $\hat{\beta}$ is isotopic to $T(2, a_1)$, $T(2, b_1)$, or the unknot respectively. The canonical fiber surface for K is produced after destabilization. The following instructions specify a construction of a branched surface for $T(2, n)$, $n \geq 3$:

$$\beta = \sigma_1^n = \sigma_1^{n-2} \quad \sigma_1 \quad \sigma_1 \\ (\rightarrow)^{n-2} \quad (\leftarrow) \quad ()$$

Standardize the disks as in Lemma 3.4. Lemmas 3.10 and 4.2, and 4.1 guarantee no product disks or band sectors are half sink disks. There are no polygon sectors. $\hat{\alpha}_1^-$ and $\hat{\alpha}_{n-1}^+$ point out of S_1 and S_2 respectively, ensuring no disk sectors. Finally, Lemma 4.3 guarantees only α_{n-2}^- and α_{n-1}^- are linked.

Thus for any $\beta = \sigma_1^{a_1} \sigma_2^{b_1}$, $a_1, b_1 \geq 1$ and odd, there exists a sink disk free branched surface B with a unique pair of linked arcs. Including both sectors induced by α_1 to τ' ensures that τ' carries all rational $r < 2g(K) - 1$. \square

Proposition 4.7. (*Building the branched surface for Type B*)

Suppose $\beta = \sigma_1^{a_1} \sigma_2 \sigma_1^{a_2} \sigma_2$, $a_i \geq 2$ and $K = \hat{\beta}$. There exists a sink-disk free branched surface $B \subset X_K$ with exactly one pair of linked arcs. Moreover, there is a sub-train-track τ' of τ carrying all rational slopes $r < 2g(K) - 1$.

Proof. The spine of the branched surface is built from $F \times \{\frac{1}{2}\}$, fused with the product disks specified below:

$$\begin{aligned} \beta &= \sigma_1^{a_1} \sigma_2 \sigma_1^{a_2} \sigma_2 \\ &= \sigma_1^{a_1} \quad \sigma_2 \quad \sigma_1^{a_2-1} \quad \sigma_1 \quad \sigma_2 \\ (4.2) \quad &= (\leftarrow)^{a_1} (\leftarrow) (\rightarrow)^{a_2-1} () () \end{aligned}$$

Lemma 3.4 puts the product disks into standardized position. Cusping the disks as specified in (4.2) yields a branched surface, as in Figure 14. By Lemma 3.10, no product disk sector is a half sink disk. No disk sectors are half sink disks:

- $\hat{\alpha}_{a_1+2}^-$ points out of the S_1 disk sector
- $\hat{\alpha}_1^-$ points into the S_1 disk sector, so $\hat{\alpha}_1^+$ points out of the S_2 disk sector
- $\hat{\alpha}_{a_1+1}^-$ points into the S_2 disk sector, so $\hat{\alpha}_{a_1+1}^+$ points out of the S_3 disk sector

Lemmas 4.1 and 4.2 guarantee no band sectors are sink disks. It remains to check the single polygon sector P , which lies in Seifert disk S_2 . The boundary of P meets α_j^+ , $a_1 + 2 \leq j \leq c_1 + c_2 - 2$, $\alpha_{a_1+1}^-$, $\alpha_{a_1}^+$, and no other arcs α_j^\pm . Since $\hat{\alpha}_{a_1+1}^-$ points out of P , it is not a half sink disk. Thus, our branched surface B is sink disk free.

We are fusing $c_1 + c_2 - 2$ product disks to $F \times \{\frac{1}{2}\}$, so there exists a sub-train-track τ' with $c_1 + c_2 - 2$ sectors. By Lemmas 4.3 and 4.4, $\alpha_{a_1}^-$ and $\alpha_{a_1+1}^-$ are the unique pair of linked arcs.

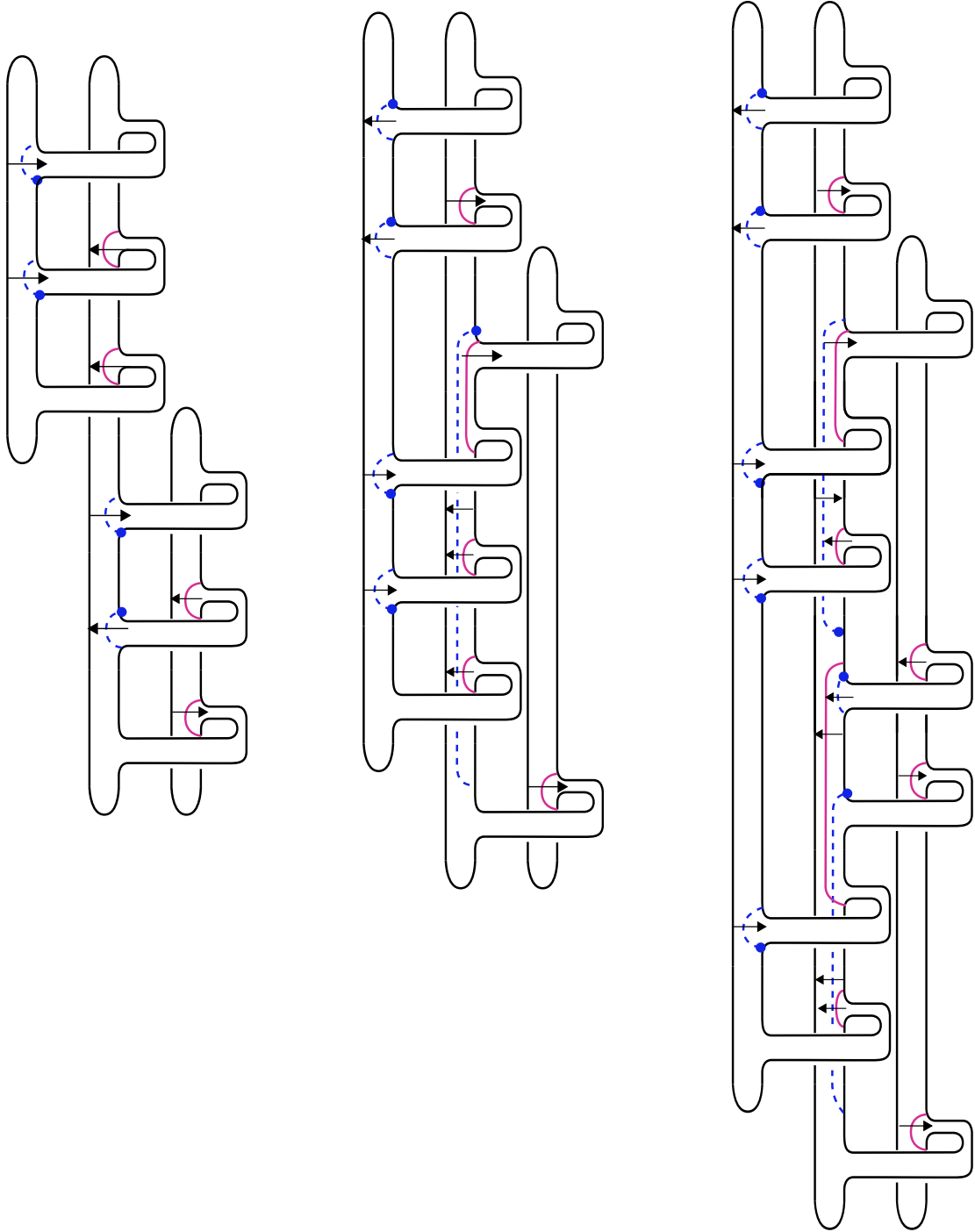


FIGURE 14. From left to right: laminar branched surfaces of Types A, B, and C.

Thus τ' carries all slopes in $[0, c_1 + c_2 - 3] = [0, 2g(K) - 1]$. Including both sectors induced by α_{a_1+1} to τ' ensures that τ' carries all slopes $r < 2g(K) - 1$. \square

The most nuanced construction arises in **Case C**:

Proposition 4.8. (*Building the branched surface for Case C*)

Let $K = \hat{\beta}$, where β is of **Case C** (see Definition 4.5). There exists a sink-disk free branched surface $B \subset X_K$ with a unique pair of linked arcs. Moreover, there is a sub-train-track τ' of τ carrying all rational slopes $r < 2g(K) - 1$.

Proof. The spine of the branched surface is built from $F \times \{\frac{1}{2}\}$, fused with the product disks specified by:

$$\begin{aligned}
 \beta &= \sigma_1^{a_1} \sigma_2^{b_1} \sigma_1^{a_2} \sigma_2^{b_2} \dots \sigma_1^{a_k} \sigma_2^{b_k} \\
 &= \sigma_1^{a_1} (\sigma_2) (\sigma_2^{b_1-1}) \sigma_1^{a_2} \sigma_2^{b_2} \sigma_1^{a_3} \sigma_2^{b_3} \dots (\sigma_1^{a_k-1}) (\sigma_1) (\sigma_2^{b_k-1}) (\sigma_2) \\
 (4.3) \quad &= (\leftarrow)^{a_1} (\rightarrow) (\leftarrow)^{b_1-1} (\rightarrow)^{a_2} (\leftarrow)^{b_2} (\rightarrow)^{a_3} (\leftarrow)^{b_3} \dots (\rightarrow)^{a_k-1} (\leftarrow) (\leftarrow)^{b_k-1} (\leftarrow)
 \end{aligned}$$

Applying Lemma 3.4 puts the product disks into standardized position. Cusping the disks as specified in (4.3) yields a branched surface B . See Figure 14 for an example.

We check for half sink disks: by Lemma 3.10, no product disk sector is a half sink disk. No disk sector is a half sink disk:

- $\hat{\alpha}_{a_1+b_1+1}^-$ points out of the S_1 disk sector
- $\hat{\alpha}_1^-$ points into the S_1 disk sector, $\hat{\sigma}_1^+$ points out of the S_2 disk sector
- whether $k = 2$ or $k = 3$, there exists a σ_2 letter in β cusped via (\leftarrow) . The corresponding image arc will point out of the S_3 disk sector

Lemmas 4.1 and 4.2 guarantee no band sectors are sink disks.

It remains to analyze polygon sectors. Unlike the cases analyzed in Propositions 4.6 and 4.7, there may be intersection points between α^+ and α^- arcs. Each intersection point will occur between consecutive blocks. Moreover, each intersection point indicates the existence of two polygon sectors. Reading from top-to-bottom, we number the intersection points $i_1, \dots, i_m, \dots, i_n$. We identify the polygon sectors by their relative position, calling them *upper polygon* and *lower polygon* sectors, and labelling them $P_{u,m}$ and $P_{\ell,m}$ respectively.

If $b_1 = 1$, we have a single polygon sector P . It is not a half sink disk, as $\hat{\alpha}_{a_1+1}^+$ points out of the region. If $b_1 \geq 2$, we have a pair of polygon sectors to analyze:

- The boundary of $P_{u,1}$ meets the arcs
 - $\alpha_j^-, a_1 + 1 \leq j \leq a_1 + b_1$
 - $\alpha_{a_1}^+$,
- The boundary of $P_{\ell,1}$ meets the arcs
 - $\alpha_{a_1+b_1}^-$,
 - $\alpha_{a_1}^+$,
 - $\alpha_j^+, a_1 + b_1 + 1 \leq j \leq a_1 + b_1 + a_2 - 1$,

Since $\hat{\alpha}_{a_1+1}^-$ points out of $P_{u,1}$, and $\hat{\alpha}_{a_1+b_1}^-$ points out of $P_{\ell,1}$, neither are half sink disks.

If, for $q \geq 2$, the q^{th} block has $b_q = 1$, there will be a single polygon region. It is not a half sink disk because $\widehat{\alpha}_{a_1+b_1+\dots+a_q}^-$ points out of it region. All remaining polygon sectors come in pairs, and can be analyzed simultaneously. For a pair $P_{u,m}$ and $P_{\ell,m}$,

- the boundary of $P_{u,m}$ meets the arcs
 - $\alpha_j^-, a_1 + b_1 + \dots + a_t + 1 \leq j \leq a_1 + b_1 + \dots + a_m + b_m$
 - $\alpha_{a_1+b_1+\dots+a_m}^+$
- The boundary of $P_{\ell,m}$ meets the arcs
 - $\alpha_{a_1+b_1+\dots+a_m+b_m}^-$
 - $\alpha_{a_1+b_1+\dots+a_m}^+$
 - $\alpha_j^+, a_1 + b_1 + \dots + b_m + 1 \leq j \leq a_1 + b_1 + \dots + b_m + a_{m+1} - 1$

For each $2 \leq t \leq k-1$, $P_{u,m}$ is not a sink disk: $\widehat{\alpha}_{a_1+b_1+\dots+a_t}^+$ points out of it. Furthermore, $P_{\ell,m}$ has $\widehat{\alpha}_{a_1+b_1+\dots+a_t+b_t}^-$ pointing out of it. Thus B is sink disk free.

We cusped $(c_1 - 1) + (c_2 - 1)$ arcs. By Lemma 4.3, there exists a single linked pair, arising from the arcs associated to the first two occurrences of σ_2 in β . Thus, there exists a sub-train-track τ' carrying all slopes in $[0, c_1 + c_2 - 3] = [0, 2g(K) - 1]$. Including the sectors induced by α_{a_1+1} to τ' ensures that τ' carries all rational $r < 2g(K) - 1$. \square

4.3. Finale. We conclude this section with the proof of the main theorem.

Proof of Theorem 1.2. Let $K \subset S^3$ be the closure of a positive 3-braid β . After isotopy, β has the form specified by Equation 2.1, and by Definition 4.5 is Type A, B or C. By Propositions 4.6, 4.7, 4.8, there exists a branched surface $B \subset X_K$ inducing a sub-train-track τ' carrying all rational slopes in the interval $(-\infty, 2g(K) - 1)$. B is laminar by Proposition 3.11; applying Theorem 2.4 yields a family of essential laminations $\{\mathcal{L}_r \mid r \in (-\infty, 2g(K) - 1) \cap \mathbb{Q}\}$, where \mathcal{L}_r meets ∂X_K in simple closed curves of slope r . Proposition 3.18 extends the essential lamination \mathcal{L}_r to a taut foliation \mathcal{F}_r in X_K , foliating ∂X_K by simple closed curves of slope r . Performing r -framed Dehn filling yields $S_r^3(K)$ endowed with a taut foliation. \square

5. PROOF OF THEOREM 1.8

We generalize the techniques developed in Sections 3 and 4 to produce taut foliations in 1-bridge braid exteriors. Gabai defines a 1-bridge braid $K(w, b, t)$ in $D^2 \times S^1$ to be a knot, realized as the closure of a positive braid β , which is specified by three parameters: w , the braid index; b , the bridge width; and t , the twist number: $\beta = (\sigma_b \sigma_{b-1} \dots \sigma_2 \sigma_1)(\sigma_{w-1} \sigma_{w-2} \dots \sigma_2 \sigma_1)^t$ where $1 \leq b \leq w-2$, $1 \leq t \leq w-2$ [Gab90]. We consider a slightly more general definition:

Definition 5.1. A 1-bridge braid K in S^3 is a knot realized as the closure of a braid β on w -strands, where

$$\beta = \underbrace{(\sigma_b \sigma_{b-1} \dots \sigma_2 \sigma_1)}_{\text{bridge subword}} (\sigma_{w-1} \sigma_{w-2} \dots \sigma_2 \sigma_1)^t$$

for $w \geq 3$, $1 \leq b \leq w-2$, $t \geq 1$. We call the first b letters of β the **bridge subword**.

In particular, we allow a 1-bridge braid in S^3 to have arbitrarily large twist number.

Remark 5.2. *There are no 1-bridge braids with $w = 3$; we may assume $w \geq 4$.*

Theorem 1.8. *Let K be a 1-bridge braid in S^3 . Then for every $r \in (-\infty, g(K)) \cap \mathbb{Q}$, the knot exterior $X_K := S^3 - \mathring{\nu}(K)$ admits taut foliations meeting the boundary torus T in parallel simple closed curves of slope r . Moreover, the manifold obtained by r -framed Dehn filling, $S_r^3(K)$, admits a taut foliation.*

Every 1-bridge braid K is a fibered knot in S^3 . As in Theorem 1.2, proving Theorem 1.8 requires building a laminar branched surface B from a copy of the fiber surface F and a collection of product disks.

Definition 5.3. *Let \mathcal{B}_w denote the braid group on w strands. Suppose $\beta' \in \mathcal{B}_w$ such that $\beta' = \sigma_m \sigma_{m-1} \sigma_{m-2} \dots \sigma_2 \sigma_1$, with $1 \leq m \leq w-1$. We call the canonical fiber surface F' for β' , built from w disks and m 1-handles, a **horizontal slice**.*

We can view the canonical fiber surface F for a 1-bridge braid $K(w, b, t)$ as built by vertically stacking $t+1$ horizontal slices, $\mathfrak{h}_0, \mathfrak{h}_1, \dots, \mathfrak{h}_{t+1}$: numbering the horizontal slices from top-to-bottom, the horizontal slice \mathfrak{h}_0 comes from the bridge subword; the remaining t horizontal slices $\mathfrak{h}_1, \dots, \mathfrak{h}_t$ come from the t occurrences of the subword $\sigma_{w-1} \sigma_{w-2} \dots \sigma_2 \sigma_1$ in β .

Definition 5.4. *A Seifert disk S_i is **odd (even)** if i is odd (even).*

As in Sections 3 and 4, we provide cusping directions in tandem with β .

Proposition 5.5. *For K a 1-bridge braid in S^3 , the following cusping directions specify a sink disk free branched surface:*

- σ_i is cusped via $(\) \iff i$ is even, or i is odd and σ_i is associated to a 1-handle used to build \mathfrak{h}_t .
- Otherwise, σ_i is cusped via (\leftarrow) or (\rightarrow) , as specified below:
 - The first occurrence of σ_i in β is cusped (\leftarrow) .
 - All other occurrences of σ_i in β are cusped via (\rightarrow) .

Proof. Following Sections 3 and 4, choose the product disks $\{D_j\}$ specified above, and build the spine for a branched surfaces from $F \times \{\frac{1}{2}\}$ and $\{D_j\}$. Applying the proof of Lemma 3.4 splits the spine of B , putting the disks in standard position. After standardizing, all α_j^- lie in odd Seifert disks S_i , and all α_j^+ lie in even Seifert disks. Choosing co-orientations for $\{D_j\}$ as specified by the instructions provided yields a branched surface B .

We check B has no sink disks. No Seifert disk S_i contains both α_j^- and α_ℓ^+ arcs, thus there are no polygon sectors. It suffices to check that no disk and band sectors are sink disks. There are at most $t+1$ band sectors: one for each horizontal slice $\mathfrak{h}_0, \mathfrak{h}_1, \dots, \mathfrak{h}_t$.

Definition 5.6. *The branch sector containing the bands in \mathfrak{h}_i is the i^{th} **band sector**, and denoted \mathbb{B}_i .*

We consider 3 cases: $t = 1$, $t = 2$, and $t \geq 3$.

If $t = 1$, then after destabilizing, $K = K(w, b, 1) \approx T(b + 1, 2) \approx T(2, b + 1)$ as knots in S^3 . In Proposition 4.6, we constructed a laminar branched surface B for any knot $K = T(2, n)$, where the induced train track τ carried all slopes $(-\infty, 2g(K) - 1)$. Appealing to Theorem 1.2 yields a stronger result than the one we seek for Theorem 1.8.

Before treating the $t = 2$ and $t \geq 3$ cases, we prove:

Lemma 5.7. *Let B be the branch surface described above, for $K(w, b, t)$ with $t \geq 2$. If b is odd (resp. even), the disk sectors S_1, \dots, S_{b+1} (resp. S_1, \dots, S_b) are not half sink disks.*

Proof. If b is odd (resp. even), then every odd Seifert disk among S_1, \dots, S_b (resp. S_1, \dots, S_{b-1}) contains arcs α_j^- cusped via both (\leftarrow) and (\rightarrow) (this is guaranteed since $t \geq 2$). Lemma 3.8 guarantees all Seifert disks S_1, S_2, \dots, S_{b+1} (resp. S_1, S_2, \dots, S_b) contain arcs cusped via both (\leftarrow) and (\rightarrow) . Each of these disks contains an outward pointing cusped arc, hence they are not half sink disks. This completes the proof of Lemma 5.7

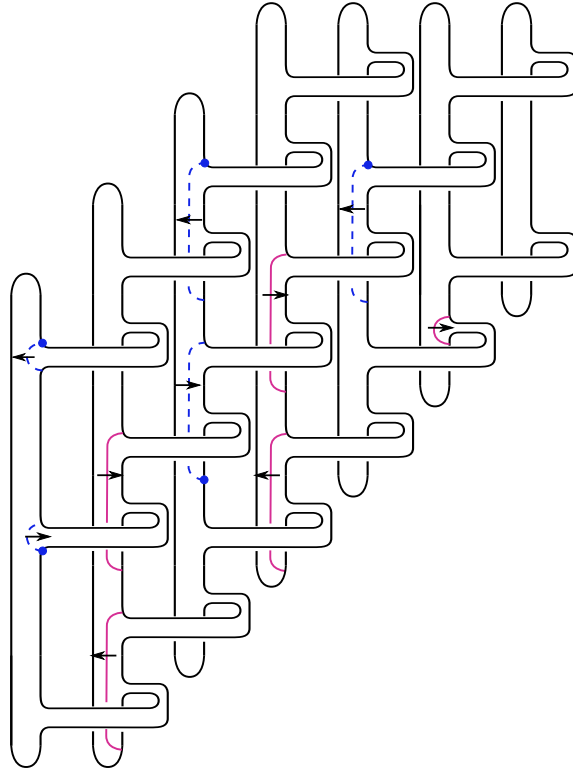


FIGURE 15. A laminar branched surface for the 1-bridge braid $K(7, 4, 2)$

We return to the proof of Proposition 5.5.

If $t = 2$, we have a three subcases:

- $b = w - 2, b \equiv w \equiv 0 \pmod{2}$

No band sectors are half sink disks: $\hat{\alpha}_b^-$, $\hat{\alpha}_{b+1}^-$, and $\hat{\alpha}_{b+w-1}^+$ point out $\mathbb{B}_0, \mathbb{B}_1$ and \mathbb{B}_2 respectively.

By Lemma 5.7, the disk sectors S_1, S_2, \dots, S_{w-2} are not half sink disks. S_{w-1}, S_{w-2} , and \mathbb{B}_1 are part of the same branch sector; we already determined \mathbb{B}_1 is not a half sink disk. Finally, $\hat{\alpha}_{b+1}^+$ points out of S_w , and B is sink disk free.

- $b = w - 2, b \equiv w \equiv 1 \pmod{2}$

No band sectors are half sink disks: $\hat{\alpha}_b^-$ and $\hat{\alpha}_{b+w-1}^+$ point out of \mathbb{B}_0 and \mathbb{B}_2 respectively. \mathbb{B}_1 and \mathbb{B}_2 are in the same branch sector, so \mathbb{B}_2 is not a half sink disk.

By Lemma 5.7, the Seifert disks S_1, S_2, \dots, S_{w-1} are not half sink disks. S_w and \mathbb{B}_2 are in the same branch sector. B is sink disk free.

- $b < w - 2$

$\hat{\alpha}_b^-$ and $\hat{\alpha}_{b+w-1}^+$ point out of \mathbb{B}_0 and \mathbb{B}_2 respectively. Either $\hat{\alpha}_{b+1}^-$ (if $w \equiv 0 \pmod{2}$) or $\hat{\alpha}_{b+2}^-$ (if $w \equiv 1 \pmod{2}$) points out of \mathbb{B}_1 . No band sectors are half sink disks.

If $b \equiv 0 \pmod{2}$, then by Lemma 5.7, S_1, S_2, \dots, S_b are not half sink disks. Every even Seifert disk S_i with $i \geq b+2$ contains an image arc cusped via (\rightarrow) . S_{b+1} is in the same branch sector as S_1 . All other Seifert disks $S_i, i \geq b+3$ are in the same branch sector as \mathbb{B}_1 , which we know has an outwardly cusped arc. B is sink disk free.

Alternatively, if $b \equiv 1 \pmod{2}$, then by Lemma 5.7, S_1, S_2, \dots, S_{b+1} are not half sink disks. Every even Seifert disk $S_i, i \geq b+3$ contains an image arc cusped via (\rightarrow) . Every odd Seifert disk $S_i, i \geq b+2$ is in the same branch sector as S_1 . B is sink disk free.

Consider a 1-bridge braid with $t \geq 3$. Every odd Seifert disk S_i contains arcs cusped via both (\leftarrow) and (\rightarrow) . If w is even (resp. odd), the proof of Lemma 5.7 guarantees S_1, \dots, S_w (resp. S_1, S_2, \dots, S_{w-1}) are not half sink disks. If w is odd, S_1 and S_w will be in the same disk sector. We conclude no disks sectors are half sink disks.

Finally, we verify no band sectors are sink disks: $\hat{\alpha}_b^-$ points out of \mathbb{B}_0 . For each $2 \leq i \leq t$, $\hat{\alpha}_{b+(i-1)(w-1)}^-$ points out of \mathbb{B}_i . We need only confirm \mathbb{B}_1 is not a half sink disk. If $b < w - 2$, $\hat{\alpha}_{b+2}^-$ points out of \mathbb{B}_1 (if w is odd) or $\hat{\alpha}_{b+1}^-$ does (if w is even). If $b = w - 2$ and $w \equiv 1 \pmod{2}$, then \mathbb{B}_1 and S_w are in the same branch sector; we know \mathbb{B}_1 is not a half sink disk. If $b = w - 2$ and $w \equiv 0 \pmod{2}$, then $\hat{\alpha}_{b+1}^-$ points out of \mathbb{B}_1 . We conclude B is sink disk free. \square

Lemma 5.8. *The train track τ , induced by B , admits no linked pairs of arcs.*

Proof. All arcs α_j^- contributing maximally to τ lie in odd Seifert disks S_i . Therefore, the only way to produce a linked pair of arcs is if σ_m^- and σ_{m+w-1}^- are cusped via (\rightarrow) and (\leftarrow) respectively, as in Figure 16. Our cusping directions avoid these instructions. \square

Definition 5.9. *Let K be a 1-bridge braid, and B the sink disk free branched surface built in Proposition 5.5. Define Γ to be the number of product disks used to build B .*

Lemma 5.10. *The induced train track τ carries all rational slopes in $(-\infty, g(K))$.*

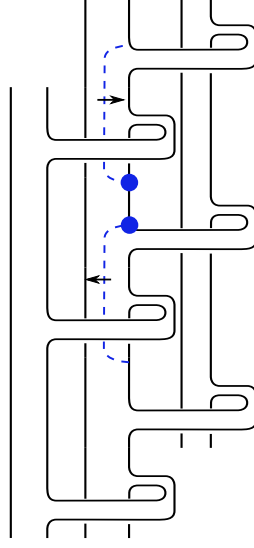


FIGURE 16. These cusping instructions for α_m^- and α_{m+w-1}^- yield a linked pair.

Proof. By Lemma 5.8, we have no linked arcs; therefore, we need only count the total number of product disks Γ used to build B , and verify $\Gamma \geq g(K)$. It is straightforward to compute the genus of any 1-bridge braid K :

$$\chi(F) = w - ((w-1)t + b) \implies g(K) = \frac{-\chi(F) + 1}{2} = \frac{wt - w - t + b + 1}{2}$$

The value of Γ depends on the parity of w and b ; we analyze the 4 possible cases below:

parity of w	parity of b	Γ
even	even	$\frac{(t-1)w}{2} + \frac{b}{2} = \frac{wt + b - w}{2}$
even	odd	$\frac{(t-1)w}{2} + \frac{b+1}{2} = \frac{wt - w + b + 1}{2}$
odd	even	$\frac{(w-1)(t-1)}{2} + \frac{b}{2} = \frac{wt - w - t + b + 1}{2}$
odd	odd	$\frac{(w-1)(t-1)}{2} + \frac{b+1}{2} = \frac{wt - w - t + b + 2}{2}$

In each case above, $\Gamma \geq g(K)$. Including both sectors of τ induced by α_b yields a sub-train track τ' carrying all slopes in $(-\infty, g(K))$. Therefore, for any K , the train track τ induced by laminar branched surface B carries all rational slopes $r < g(K)$. \square

Proof of Theorem 1.8. By Propositions 5.5 and 3.11, for any 1-bridge braid $K \subset S^3$, there exists a laminar branched surface $B \subset X_K$. By Lemma 5.10, the boundary train track τ carries all rational slopes $r < g(K)$. Applying Theorem 2.4 yields a family of essential laminations \mathcal{L}_r carried by B , where $r < g(K)$. Proposition 3.18 extends each essential lamination \mathcal{L}_r to a taut foliation \mathcal{F}_r meeting ∂X_K in simple closed curves of slope r . Performing r -framed Dehn filling produces $S_r^3(K)$ endowed with a taut foliation. \square

REFERENCES

- [Ber18] John Berge, *Some knots with surgeries yielding lens spaces*, <https://arxiv.org/abs/1802.09722> (2018).
- [Bow16] Jonathan Bowden, *Approximating C^0 -foliations by contact structures*, *Geom. Funct. Anal.* **26** (2016), no. 5, 1255–1296.
- [BC15] Steven Boyer and Adam Clay, *Slope detection, foliations in graph manifolds, and L-spaces*, <https://arxiv.org/abs/1510.02378> (2015).
- [BC17] Steven Boyer and Adam Clay, *Foliations, orders, representations, L-spaces and graph manifolds*, *Adv. Math.* **310** (2017), 159–234.
- [BGW13] Steven Boyer, Cameron McA. Gordon, and Liam Watson, *On L-spaces and left-orderable fundamental groups*, *Math. Ann.* **356** (2013), no. 4, 1213–1245.
- [BNR97] Mark Brittenham, Ramin Naimi, and Rachel Roberts, *Graph manifolds and taut foliations*, *J. Differential Geom.* **45** (1997), no. 3, 446–470.
- [CLW13] Adam Clay, Tye Lidman, and Liam Watson, *Graph manifolds, left-orderability and amalgamation*, *Algebr. Geom. Topol.* **13** (2013), no. 4, 2347–2368.
- [DR] Charles Delman and Rachel Roberts, *Personal communication*.
- [EHN81] David Eisenbud, Ulrich Hirsch, and Walter Neumann, *Transverse foliations of Seifert bundles and self-homeomorphism of the circle*, *Comment. Math. Helv.* **56** (1981), no. 4, 638–660.
- [FS80] Ronald Fintushel and Ronald J. Stern, *Constructing lens spaces by surgery on knots*, *Math. Z.* **175** (1980), no. 1, 33–51.
- [FO84] W. Floyd and U. Oertel, *Incompressible surfaces via branched surfaces*, *Topology* **23** (1984), no. 1, 117–125.
- [Gab83] David Gabai, *Foliations and the topology of 3-manifolds*, *J. Differential Geom.* **18** (1983), no. 3, 445–503.
- [Gab85] ———, *The Murasugi sum is a natural geometric operation. II*, *Combinatorial methods in topology and algebraic geometry* (Rochester, N.Y., 1982), *Contemp. Math.*, vol. 44, Amer. Math. Soc., Providence, RI, 1985, pp. 93–100.
- [Gab86] ———, *Detecting fibred links in S^3* , *Comment. Math. Helv.* **61** (1986), no. 4, 519–555.
- [Gab90] ———, *1-bridge braids in solid tori*, *Topology Appl.* **37** (1990), no. 3, 221–235.
- [GO89] David Gabai and Ulrich Oertel, *Essential laminations in 3-manifolds*, *Ann. of Math. (2)* **130** (1989), no. 1, 41–73.
- [GLV18] Joshua Evan Greene, Sam Lewallen, and Faramarz Vafaee, *(1, 1) L-space knots*, *Compos. Math.* **154** (2018), no. 5, 918–933.
- [HRRW15] Jonathan Hanselman, Jacob Rasmussen, Sarah Dean Rasmussen, and Liam Watson, *Taut foliations on graph manifolds*, <https://arxiv.org/abs/1508.05911> (2015).
- [Juh15] András Juhász, *A survey of Heegaard Floer homology*, *New ideas in low dimensional topology*, Ser. Knots Everything, vol. 56, World Sci. Publ., Hackensack, NJ, 2015, pp. 237–296.

- [KR17] William H. Kazez and Rachel Roberts, C^0 approximations of foliations, *Geom. Topol.* **21** (2017), no. 6, 3601–3657.
- [KMOS07] P. Kronheimer, T. Mrowka, P. Ozsváth, and Z. Szabó, *Monopoles and lens space surgeries*, *Ann. of Math.* (2) **165** (2007), no. 2, 457–546.
- [LV14] Cristine Lee and Faramarz Vafaee, *On 3-braids and L-space knots*, <https://tinyurl.com/ycshfx7s> (2014).
- [Li02] Tao Li, *Laminar branched surfaces in 3-manifolds*, *Geom. Topol.* **6** (2002), 153–194.
- [Li03] ———, *Boundary train tracks of laminar branched surfaces*, *Topology and geometry of manifolds* (Athens, GA, 2001), *Proc. Sympos. Pure Math.*, vol. 71, Amer. Math. Soc., Providence, RI, 2003, pp. 269–285.
- [LM16] Tye Lidman and Allison H. Moore, *Pretzel knots with L-space surgeries*, *Michigan Math. J.* **65** (2016), no. 1, 105–130.
- [LS09] Paolo Lisca and András I. Stipsicz, *On the existence of tight contact structures on Seifert fibered 3-manifolds*, *Duke Math. J.* **148** (2009), no. 2, 175–209.
- [Nie18] Zipei Nie, *Left-orderability for surgeries on $P(-2, 3, 2s + 1)$ pretzel knots*, <https://arxiv.org/abs/1803.00076> (2018).
- [OS04] Peter Ozsváth and Zoltán Szabó, *Holomorphic disks and genus bounds*, *Geom. Topol.* **8** (2004), 311–334.
- [OS05] ———, *On knot Floer homology and lens space surgeries*, *Topology* **44** (2005), no. 6, 1281–1300.
- [RR17] Jacob Rasmussen and Sarah Dean Rasmussen, *Floer simple manifolds and L-space intervals*, *Adv. Math.* **322** (2017), 738–805.
- [Rob01a] Rachel Roberts, *Taut foliations in punctured surface bundles. I*, *Proc. London Math. Soc.* (3) **82** (2001), no. 3, 747–768.
- [Rob01b] ———, *Taut foliations in punctured surface bundles. II*, *Proc. London Math. Soc.* (3) **83** (2001), no. 2, 443–471.
- [Rud93] Lee Rudolph, *Quasipositivity as an obstruction to sliceness*, *Bull. Amer. Math. Soc. (N.S.)* **29** (1993), no. 1, 51–59.
- [Sta78] John R. Stallings, *Constructions of fibred knots and links*, *Algebraic and geometric topology* (Proc. Sympos. Pure Math., Stanford Univ., Stanford, Calif., 1976), Part 2, *Proc. Sympos. Pure Math.*, XXXII, Amer. Math. Soc., Providence, R.I., 1978, pp. 55–60.
- [Tra18] Anh T. Tran, *Left-orderability for surgeries on twisted torus knots*, <https://arxiv.org/abs/1809.01250> (2018).
- [Vaf15] Faramarz Vafaee, *On the knot Floer homology of twisted torus knots*, *Int. Math. Res. Not. IMRN* (2015), no. 15, 6516–6537.

DEPARTMENT OF MATHEMATICS, BOSTON COLLEGE, CHESTNUT HILL, MA 02467

E-mail address: siddhi.krishna@bc.edu